05

# Theory of the structure of icosahedral quasicrystals: types of packings

© A.E. Madison,[1] P.A. Madison[1,2]

[1] National Research University „Higher School of Economics“,
190121 St. Petersburg, Russia
[2] St. Petersburg State Electrotechnical University „LETI“,
197022 St. Petersburg, Russia
e-mail: alex_madison@mail.ru

*Received September 8, 2024*
*Revised November 20, 2024*
*Accepted November 29, 2024*

A unified theory of the structure of icosahedral quasicrystals is proposed. All possible variants of self-similar icosahedral packings are analyzed. These include 3 types of quasilattices ($P$, $I$, $F$), which are the analogues of primitive, body-centered and face-centered cubic lattices; each of them can be either centrosymmetric or non-centrosymmetric. Substitution rules for $I$ and $F$-type tetrahedral tilings are fully formalized. An example of constructing a non-centrosymmetric $I$-type packing is presented. A method is shown for generating a zonohedral packing ($P$) from a tetrahedral packing ($I$) by joining the neighboring tetrahedra in it. For each packing type, 3 locally isomorphic patches are possible, differing in the choice of node in its center (A, B, C). When the tetrahedral packings are built up, three locally isomorphic patches cyclically transform into each other after each iteration. As a consequence, the structures of the three types of characteristic clusters are not independent. An icosahedral packing of any type can be constructed based on a unified algorithm when initialized with a single tetrahedron.

**Keywords:** icosahedral quasicrystals, substitution rules, packings.

DOI: 10.61011/TP.2025.01.60508.269-24

## Introduction

The present work continues a series of works on the theory of the structure of icosahedral quasicrystals [1,2]. Higher-dimensional approach (in particular, the *cut-and-project* method) is generally accepted today when describing the structure of quasicrystals. It is based on the synthesis of Fourier series for a certain periodic distribution in a six-dimensional space based on data from a diffraction experiment, identifying it with the distribution of certain six-dimensional „atoms“ and projecting a strip cut out of it in a certain way into the physical 3$D$-space [3,4]. As discussed earlier in Ref. [2], the problems that arise in this case lead to the identification of several different clusters with one averaged structure at once, loss of precise icosahedral symmetry and violation of self-similarity. The theory of the structure of quasicrystals in its modern form is not devoid of internal contradictions, including fundamental ones. Let us quote the monograph [5]: „A three-dimensional atom has a certain pedestrian reality that does not so easily lend itself to a mapping onto six dimensions“.

The projection method is usually contrasted with the method based on the tiling theory [6,7], which, generally speaking, is not clear. After all, both of the most significant tilings (the Socolar-Steinhardt zonohedral tiling [8] and the Danzer tetrahedral tiling [9,10]) are themselves also obtained by projection from 6$D$-space.

Socolar and Steinhardt showed that if the tiling we are interested in satisfies the Penrose local isomorphism property, then it should not contain the oblate rhombohedra. In particular, the basis set can consist of 4 golden zonohedra [8]. They have also shown that there are exactly 3 perfect packings with icosahedral point symmetry in Euclidean space. As a result, three types of icosahedral clusters should be expected to appear in the real structure. In practice, on the contrary, the tiling into prolate and oblate rhombohedra is much more often used (Ammann-Kramer-Neri tiling) [11]. Incomplete or mixed sets of cells [12,13] or an overlapping cluster model are also used [14], whose theoretical validity is controversial. As a result, when elucidating the real structures, it is possible to identify either just one or, at best, two types of characteristic clusters [15,17].

There are 3 types of icosahedral quasicrystals — $P$, $I$ and $F$ (by analogy with primitive, body-centered and face-centered cubic crystals) [18,19]. It is proved that the self-similarity factor for quasilattices of all three types should be equal to $\tau^3$, and the inflation factor should be equal to $\tau$ for $I$ and $F$-types and $\tau^3$ for $P$-type, where $\tau$ is the golden ratio [20,21]. In essence, this fact reflects the property of self-similarity; it is a direct consequence of the periodicity of the cubic 6$D$-lattice from which the projection is performed. It is believed that the vast majority of the experimentally determined structures of icosahedral quasicrystals correspond to the $F$-type. However, we are not aware of any work that would verify the conformance of the analyzed structures with the required inflation parameters. It is believed [10] that the Danzer tiling is completely equivalent to the Socolar-Steinhardt tiling, but this statement surely cannot be true. As we showed earlier in Refs. [22,23],

they are characterized by different inflation factors, which is possible only if they correspond to different types of quasilattices.

The presence of contradictions prompted us to develop a theory of the structure of quasicrystals based on the tiling theory and the concept of unit cells [24]. Establishing an exact correspondence between three types of icosahedral quasicrystals ($P$, $I$, $F$) and three types of tilings (zonohedral and two tetrahedral) [1] made it possible to describe all possible variants of icosahedral packings within the framework of a single mutually agreed approach. The general principles of this approach were outlined in the 1st part of the paper [2]. The specifics of constructing icosahedral packings and clusters for each of the possible types of quasilattices are explained in detail below.

## 1. Symmetry analysis

The general principles of packing construction are common for both icosahedral and a wide variety of axial quasicrystals [25]. In particular, the value of the inflation factor is uniquely determined by the fact that the inflation symmetry of the quasicrystalline 3$D$-tiling is a consequence of the symmetry of the $n$-dimensional generating lattice [20]. In other words, after changing the scale, all the resulting quasilattice nodes should be projections of the nodes of the generating lattice.

The entire structure of an icosahedral quasicrystal is generally considered by us as a list of cells [24]. It is necessary to specify its type for each cell, as well as its position and orientation in space. Then it is necessary to specify a method for filling cells with specific atoms, taking into account their intrinsic symmetry and local matching rules, in order to ensure the correct „cross-linking“ of neighboring cells of different types into a single whole. The local symmetries of the cells and their possible orientations are determined by the methods of group theory based on the orbit-stabilizer theorem.

It is not enough for us to know the substitution matrix to formally write down the substitution rules. For each of the cells of the corresponding basis set, it is necessary to select a local coordinate system and place the cell in it, taking one of the possible orientations as the standard one. The identity element of the symmetry group will now correspond to this orientation. Any other orientation will be set by a certain symmetry element (or by a whole class of left conjugate elements with respect to the stabilizer subgroup, if the proper symmetry of the cell is not trivial). The position of the cell in space will be set by shifting the local coordinate system of the cell relative to the global coordinate system of the packing. It is enough to know the multiplication matrix of the corresponding symmetry group in order to build a cell packing, but the exact coordinate representations of matrices of specific symmetry elements are necessary to determine the positions of atoms.

The rotation group of the icosahedron $I$ has order 60 and is isomorphic to the alternating group $A_5$. The complete icosahedral group $I_h$ is formed by adding the inversion center to the group $I$, has order 120, and is isomorphic to the symmetric group $S_5$. Unfortunately, there is no single approach to numbering the elements of these groups in the literature. It depends on whether we are talking about an abstract mathematical group of permutations or a group of symmetry elements of an icosahedron, whether the elements are distributed among conjugacy classes, or whether the numbering is carried out according to the degrees of the group generators, etc. Moreover, 2 different coordinate axis settings are possible differing by a rotation by 90° relative to one of the 2-fold axes.

When choosing the orientation of the icosahedron and the numbering scheme of its vertices, we follow the study in Ref. [26] (see Fig. 1). We use generally accepted notation for the symmetry elements, but we specify in parentheses through which vertex, face or edge the axis of interest passes for their unambiguous identification [27]. The symmetry elements, sorted according to their conjugacy classes, are shown in the list (1).

For example, the 5-fold axis is designated either as $C_5$ when using Schoenflies notations, or by the symbol 5 when Hermann-Mauguin standard international notations are used. Then, taking into account the clarifications, $C_5(1)$ or $5(1)$ is the 5-fold axis passing through the vertex number 1. Similarly, $3(132)$ is a 3-fold axis passing through the face $\triangle 132$ and cyclically interchanging its vertices: $1\rightarrow3\rightarrow2$. This order of permutations is explained by the fact that we take counterclockwise rotation as the positive direction of rotation when looking at the icosahedron from the outside. Element $2(12)$ is a 2-fold axis passing through the edge [12] and swapping its vertices $1\rightarrow2$.

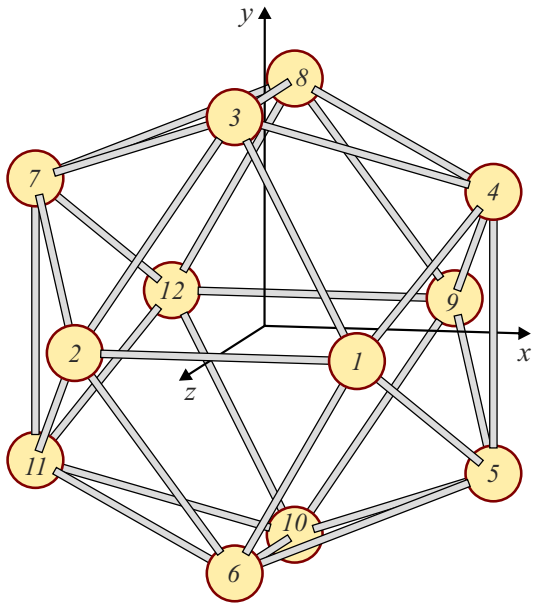


**Figure 1.** Numbering of the icosahedron vertices.

$$I_h = \left\{ \begin{array}{l} \left. \begin{array}{l} E = \{1\}, \\ 12C_5 = \{5(1),\ 5(2),\ 5(3),\ 5(4),\ 5(5),\ 5(6),\ 5^4(1),\ 5^4(2),\ 5^4(3),\ 5^4(4),\ 5^4(5),\ 5^4(6)\}, \\ 12C_5^2 = \{5^2(1),\ 5^2(2),\ 5^2(3),\ 5^2(4),\ 5^2(5),\ 5^2(6),\ 5^3(1),\ 5^3(2),\ 5^3(3),\ 5^3(4),\ 5^3(5),\ 5^3(6)\}, \\ 20C_3 = \{3(132),\ 3(143),\ 3(154),\ 3(165),\ 3(126),\ 3(237),\ 3(387),\ 3(348),\ 3(498),\ 3(459), \\ \quad 3^2(132),\ 3^2(143),\ 3^2(154),\ 3^2(165),\ 3^2(126), \\ \quad 3^2(237),\ 3^2(387),\ 3^2(348),\ 3^2(498),\ 3^2(459)\}, \\ 15C_2 = \{2(12),\ 2(13),\ 2(14),\ 2(15),\ 2(16),\ 2(23),\ 2(34),\ 2(45),\ 2(56),\ 2(26), \\ \quad 2(27),\ 2(37),\ 2(38),\ 2(48),\ 2(49)\}, \end{array} \right\} = I \\ \left. \begin{array}{l} C_i = \{\overline{1}\}, \\ 12S_{10}^3 = \{\overline{5}(1),\ \overline{5}(2),\ \overline{5}(3),\ \overline{5}(4),\ \overline{5}(5),\ \overline{5}(6),\ \overline{5}^9(1),\ \overline{5}^9(2),\ \overline{5}^9(3),\ \overline{5}^9(4),\ \overline{5}^9(5),\ \overline{5}^9(6)\}, \\ 12S_{10} = \{\overline{5}^7(1),\ \overline{5}^7(2),\ \overline{5}^7(3),\ \overline{5}^7(4),\ \overline{5}^7(5),\ \overline{5}^7(6),\ \overline{5}^3(1),\ \overline{5}^3(2),\ \overline{5}^3(3),\ \overline{5}^3(4),\ \overline{5}^3(5),\ \overline{5}^3(6)\}, \\ 20S_6 = \{\overline{3}(132),\ \overline{3}(143),\ \overline{3}(154),\ \overline{3}(165),\ \overline{3}(126),\ \overline{3}(237),\ \overline{3}(387),\ \overline{3}(348),\ \overline{3}(498),\ \overline{3}(459), \\ \quad \overline{3}^5(132),\ \overline{3}^5(143),\ \overline{3}^5(154),\ \overline{3}^5(165),\ \overline{3}^5(126), \\ \quad \overline{3}^5(237),\ \overline{3}^5(387),\ \overline{3}^5(348),\ \overline{3}^5(498),\ \overline{3}^5(459)\}, \\ 15\sigma = \{m(38),\ m(49),\ m(37),\ m(48),\ m(27),\ m(15),\ m(16),\ m(12),\ m(13),\ m(14), \\ \quad m(34),\ m(26),\ m(45),\ m(23),\ m(56)\}. \end{array} \right\} \end{array} \right. \quad (1)$$

Elements 1 and $\overline{1}$ are the identity element and the inversion, respectively.

The first 60 elements are the pure (proper) rotations. They form a group $I$. The remaining 60 elements are improper rotations (operations with negative determinant equal to $-1$), i.e. inversion itself, rotoinversions (or their corresponding rotoreflections) and mirror reflection planes. We would like to remind that improper symmetry elements change the right coordinate system to the left, and also replace the external normals of the faces with the internal ones if they are defined as the vector product of the edges forming these faces. This should be taken into account when drawing the cells in the resulting packing later.

We intentionally numbered the elements in such a way that the composition of any element of the group $I$ with an inversion would give an element whose number would be exactly 60 more. For example, the composition of the 2nd element $5(1)$ with inversion gives 62nd element in the list — the rotoinversion axis $\overline{5}$ passing through vertex 1: $\overline{5}(1) = \overline{1} \cdot 5(1)$. Similarly, the composition of the 26th element $3(132)$ with an inversion gives the 86th element in the list — the rotoinversion axis $\overline{3}$ passing through the face $\triangle 132$: $\overline{3}(132) = \overline{1} \cdot 3(132)$. To determine the permutation performed by specific rotoinversion, it is necessary to double the cycle length of the generating element (132132), and then replace the numbers at even positions (1*2*3*) with the numbers of opposite vertices. The result is a permutation: 1→10→2→12→3→9. The composition of the 46th element $2(12)$ with an inversion gives the 106th element in the list — a mirror reflection plane mapping the vertices 3→8 into each other: $m(38) = \overline{1} \cdot 2(12)$.

A complete list of all symmetry elements is provided in the Appendix to avoid any discrepancies. The elements are distributed among the conjugace classes, 120 elements form a group $I_h$. The corresponding vertex permutations and rotation matrices are given for each element.

Now we can proceed to a detailed explanation of the algorithms for constructing all possible variants of icosahedral packings.

## 2. Packings of $I$ and $F$-types

Let us summarize the conclusions drawn in the previous part of the paper [1,2,24]. Icosahedral quasilattices of all three types ($P$, $I$, $F$) are packings of unit cells. The choice of a basis set of cells is not arbitrary. Their shape is derived by projecting the Voronoi polyhedron of the corresponding $6D$-lattice. The set of zonohedra for the quasilattice of $P$-type is obtained by projecting the elementary $6D$-hypercube of the integer lattice $Z^6$, and the sets of tetrahedra for $I$ and $F$-types are obtained from the root polytope of the root lattice $D_6$. The properties of various higher-dimensional lattices and the notations used for them are described in detail in the monograph [28].

The centering scheme of $F$-type includes all nodes corresponding to $I$-type as a subset in spaces of even dimensions. As a result, the cell sets and substitution rules for all three types should be completely consistent. New nodes are added to the quasilattice of $P$-type to form a quasilattice of $I$-type, to which new nodes are added to form a quasilattice of $F$-type. In this case, the zonohedra are dissected into the tetrahedra, which, in turn, are once again dissected into the tetrahedra of a slightly different basis set.

Thus, the construction of any possible variant of a self-similar icosahedral packing is based on the joint use of three mutually consistent tilings, for each of which there are its own basis set of unit cells and its own substitution rules.

A quasilattice of $P$-type corresponds to the Socolar-Steinhardt tiling into four types of zonohedra

$\{GR, RD, RI, RT\}$. The quasilattice of $F$-type corresponds to the Danzer tiling. The standard procedure for its construction is described in Refs. [29,30]. We replace the basis tetrahedra $\{A, B, C, K\}$ [9] with their copies reduced by $\tau$ times $\{a, b, c, k\}$ to meet the requirement of mutual consistency. This procedure is not limited to a trivial change in scale, since it is also accompanied by a change in the types of nodes at the vertices of the tetrahedra. A quasilattice of $I$-type corresponds to another tetrahedral tiling, the basis set of which is formed by three copies of Danzer tetrahedra reduced by $\tau$ times and another tetrahedron of the original size — $\{a, c, k, K\}$. The latter tiling was mentioned in a single line in Danzer's seminal work [9], but no one has paid proper attention to it since. Its fundamental importance as a packing of $I$-type was indicated by us [1].

It is important to choose the correct standard cell orientations. The choice was quite obvious for all cells except the tetrahedron $a$. The fact is that 3 out of 4 tetrahedra are subsequently used to form the starting configurations in both basis sets. The corresponding vertex of the tetrahedron is aligned with the origin of the global coordinate system of the future packing. In the case of the group $I_h$, using the group action on a cell, we get 120 copies of it — a complete orbit. Combined together, they form a polyhedron with exact icosahedral symmetry — a possible starting configuration. In this case, all the edges coming out of the central node turn out to be the symmetry axes of the icosahedron — 2, 3 and 5-fold ones. We found it natural to orient the tetrahedra relative to the coordinate system of the icosahedron. We would like to emphasize that our choice differs from the one accepted in the literature [29].

Let us choose the standard orientation for 3 tetrahedra out of 4 in such a way so that the corresponding initial vertex would coincide with the origin of the local coordinate system of the cell; the edge parallel to the 2-fold axis would be directed along the $x$-axis; the edge parallel to the 5-fold axis would lie in the $(x - y)$ plane; the edge parallel to the 3-fold axis would lie in the $(x - z)$ plane; the coordinates of all the vertices will be non-negative in this case. The edge parallel to the 2-fold axis for the tetrahedron $a$ will be also directed along the $x$-axis, and the orientation will be chosen so that the coordinates of all vertices are non-negative. This choice turns out to be convenient when formulating a universal packing generation algorithm, but it will require some correction when considering right and left enantiomorphic forms.

The coordinates of the vertices of the Danzer tetrahedra in the orientations assumed by us as the standard ones are listed in Table 1. We use dimensionless values for the coordinates of the vertices. The vertex type is specified for each vertex (A, B, C, F). We use a Roman font for vertices, and an italic font for Danzer tetrahedra $(A, B, C, K)$ and Levitov packing types $(P, I, F)$ to avoid confusion when symbols match in the accepted notations (for explanations, see Ref. [2]).

Let us pay attention to an important property of all Danzer tetrahedra — all their edges are parallel to one

**Table 1.** Danzer tetrahedra

| Type of tetrahedron | Type and coordinates of vertices | Included in basis set |
|---|---|---|
| $a$ | A (0, 0, 0)<br>A (2, 0, 0)<br>C $(1+\tau,\ \tau,\ 0)$<br>B $(1,\ 0,\ \tau)$ | $I$, $F$ |
| $b$ | C (0, 0, 0)<br>C (2, 0, 0)<br>A $(1+\tau,\ \tau,\ 0)$<br>B $(1+\tau,\ 0,\ 1)$ | $F$ |
| $c$ | B (0, 0, 0)<br>B $(2\tau,\ 0,\ 0)$<br>A $(\tau,\ 1,\ 0)$<br>C $(1+\tau,\ 0,\ 1)$ | $I$, $F$ |
| $k$ | A (0, 0, 0)<br>F $(\tau,\ 0,\ 0)$<br>B $(\tau,\ 1,\ 0)$<br>C $(\tau,\ 0,\ -1+\tau)$ | $I$, $F$ |
| $K$ | C (0, 0, 0)<br>F $(1+\tau,\ 0,\ 0)$<br>A $(1+\tau,\ \tau,\ 0)$<br>B $(1+\tau,\ 0,\ 1)$ | $I$ |

of the symmetry axes of an icosahedron (2, 3 or 5-fold ones), and the normals to all faces are always parallel to the 2-fold axes. The coordinates of all vertices belong to the ring of quadratic integers of the field $\mathbb{Q}\left(\sqrt{5}\right)$. Therefore, the coordinates of all the nodes of the packing constructed from them will also be quadratic integers [31].

As noted above, unlike the Socolar-Steinhardt tiling into zonohedra, for which the inflation factor is $\tau^3$, the inflation factor for both tilings into Danzer tetrahedra is $\tau$. Therefore, the packing generation algorithm remains virtually unchanged, it is only necessary to replace the inflation multiplier:

$$\mathbf{R}_k = \tau \mathbf{R}_i + g_i \mathbf{R}_j,$$
$$g_k = g_i g_j. \qquad (2)$$

Here, as in the case of zonohedral packing [24,27], $\mathbf{R}_i$ and $g_i$ denote the position and orientation of the generating (parent) cell, $\mathbf{R}_j$ and $g_j$ denote the position and orientation of the generated (daughter) cell in the deflation scheme of the parent cell in its standard orientation, and $\mathbf{R}_k$ and $g_k$ denote the position and orientation of the generated cell, but in a global packing.

There is another significant difference related to the cyclic change of node types at each iteration: C→B→A→C. It will be explained below.

The construction of an icosahedral packing of $I$-type based on a tetrahedral $ackK$-tiling is illustrated in Fig. 2. The figure above shows 4 tetrahedra $\{a, c, k, K\}$ oriented

**Table 2.** Substitution rules for packing of $I$-type

| № $j$ | Type of cell | Position $\mathbf{R}_j$ | Orientation № | Orientation $g_j$ |
|---|---|---|---|---|
| | | $a \to \mathrm{infl}(a)$ | | |
| 1 | $K$ | (0, 0, 0) | 1 | 1 |
| 2 | $K$ | (0, 0, 0) | 111 | $m(15)$ |
| 3 | $K$ | (0, 0, 0) | 28 | $3(154)$ |
| 4 | $k$ | $(1+\tau, \tau, 0)$ | 104 | $\overline{3}^5(498)$ |
| 5 | $k$ | $(1+\tau, \tau, 0)$ | 20 | $5^3(1)$ |
| 6 | $k$ | $(\tau, 0, 1+\tau)$ | 102 | $\overline{3}^5(387)$ |
| 7 | $c$ | $(1+2\tau, 1+\tau, 0)$ | 54 | $2(56)$ |
| 8 | $c$ | $(1+2\tau, 1+\tau, 0)$ | 77 | $\overline{5}^7(4)$ |
| | | $K \to \mathrm{infl}(K)$ | | |
| 1 | $c$ | (0, 0, 0) | 1 | 1 |
| 2 | $k$ | $(\tau, 1, 0)$ | 76 | $\overline{5}^7(3)$ |
| 3 | $k$ | $(1+2\tau, 0, \tau)$ | 55 | $2(26)$ |
| 4 | $K$ | $(1+2\tau, 1+\tau, 0)$ | 54 | $2(56)$ |
| 5 | $K$ | $(1+2\tau, 1+\tau, 0)$ | 63 | $\overline{5}(2)$ |
| 6 | $K$ | $(1+2\tau, 1+\tau, 0)$ | 41 | $3^2(237)$ |
| | | $c \to \mathrm{infl}(c)$ | | |
| 1 | $k$ | (0, 0, 0) | 1 | 1 |
| 2 | $k$ | $(2\tau, 0, 0)$ | 113 | $m(12)$ |
| 3 | $c$ | $(1+2\tau, 0, \tau)$ | 55 | $2(26)$ |
| 4 | $c$ | $(1+2\tau, 0, \tau)$ | 66 | $\overline{5}(5)$ |
| 5 | $a$ | $(2+2\tau, 0, 0)$ | 113 | $m(12)$ |
| | | $k \to \mathrm{infl}(k)$ | | |
| 1 | $K$ | (0, 0, 0) | 1 | 1 |

relative to the symmetry axes of an icosahedron. The coordinates of the vertices are specified for such particular orientation in Table 1. We took it for the standard one. Nodes of different types are marked with different colors: A (white), B (black), C (red), F (turquoise). Since there are 2 types of edges [AB] of the same length, the edges of the 2nd type are also highlighted by color (for explanations, see [1]). The order of writing out tetrahedra in both basis sets was adopted by Danzer [9]: $\{A, B, C, K\}$ and $\{A, C, K, \tau K\}$, after rescaling we get $\{a, b, c, k\}$ and $\{a, c, k, K\}$, respectively. In the Fig. 2, the enlarged tetrahedron $K$ is placed second to emphasize the fact that it is used instead of $b$ in the second basis set. The second row contains substitution rules: tetrahedra increase by a factor of $\tau$ and are made up of tetrahedra of the original size. The substitution rules, written as lists of cells, are given in Table 2.

Next, Fig. 2 shows the substitution rules in the form of polyhedron packings. A single tetrahedron can be used to initialize the algorithm for constructing the entire packing. In total, there are 3 locally isomorphic packing variants (centered at nodes A, B, C). By acting on the corresponding tetrahedron by all elements of the symmetry group of the icosahedron, we obtain 120 copies of it united in the starting configuration. After applying the 1st iteration, we obtain a fragment of the packing in the form of a polyhedron of the initial configuration, but enlarged by $\tau$ times.

Let us now explain the property associated with the cyclic change of node types at each iteration: C→B→A→C. All nodes are being changed, including the central ones. Applying the inflation and deflation to the starting configuration of packing C (a triacontahedron of 120 tetrahedra $K$) results not in the adding of the next layer to the initial starting configuration (as it would be intuitively expected), but in a patch of packing B in the form of a the triacontahedron enlarged by $\tau$ times. In other words, applying the next iteration to packing C turns it into packing B. Applying another iteration to packing B turns it into packing A. Applying another iteration to packing A turns it into packing C.

The loop closes after three iterations: C→B→A→C. We can draw 3 important conclusions. Firstly, the inflation factor of the substitution algorithm is $\tau$ whereas the self-similarity factor of the packing is $\tau^3$. Secondly, any of the three packing variants can be constructed from a single tetrahedron. Any tetrahedron can act as such except for $a$. Thirdly, the structure of the characteristic clusters located at nodes A, B, and C is interrelated. In particular, if in the structure of an ideal icosahedral quasicrystal the nodes A and B form a triacontahedron around node C, then C and A form a $\tau$ times larger triacontahedron around B, and B and C form a $\tau^2$ times larger triacontahedron around A.

As to the software implementation, it is first necessary to set a starting cell (or a small starting cluster of several cells, see below). For example, we start building a packing centered at node A. The starting cell is the tetrahedron $k$. The entire packing consists of a single cell at this stage of the algorithm and the list of cells consists of a single row: cell type $k$, position (0, 0, 0), orientation 1 (the identity transformation). Now we have to multiply the starting cell by the symmetry group $I_h$, so we get a starting configuration in the form of a triacontahedron of 120 tetrahedra $k$. The list of cells will then contain 120 rows: the type of all cells $k$, the position of all cells is set by the vector (0, 0, 0), but the orientations are all different — from 1 to 120 (the full orbit of the cell). The initialization stage is completed, and now we can proceed to the iterative algorithm of inflation and deflation.

At this stage, we move each time through the list of cells, which is generated in the previous iteration. The appropriate rule is selected from Table 2 for each cell in the list depending on its type, and a new cluster of appropriately oriented cells is generated in a particular place according to the equations (2). In particular, a list of 120 tetrahedra $k$ (a triacontahedron centered at node A) generates a new list of 120 tetrahedra $K$ (the $\tau$ times enlarged triacontahedron centered at node C). This transformation is marked by a curved arrow from A to C in Fig. 2. Let us proceed to the next iteration. Each of the 120 tetrahedra $K$ generates 6 new tetrahedra according to Table 2 and equations (2). The result is the $\tau^2$ times enlarged triacontahedron centered at node B. The starting configuration for node B is inside:

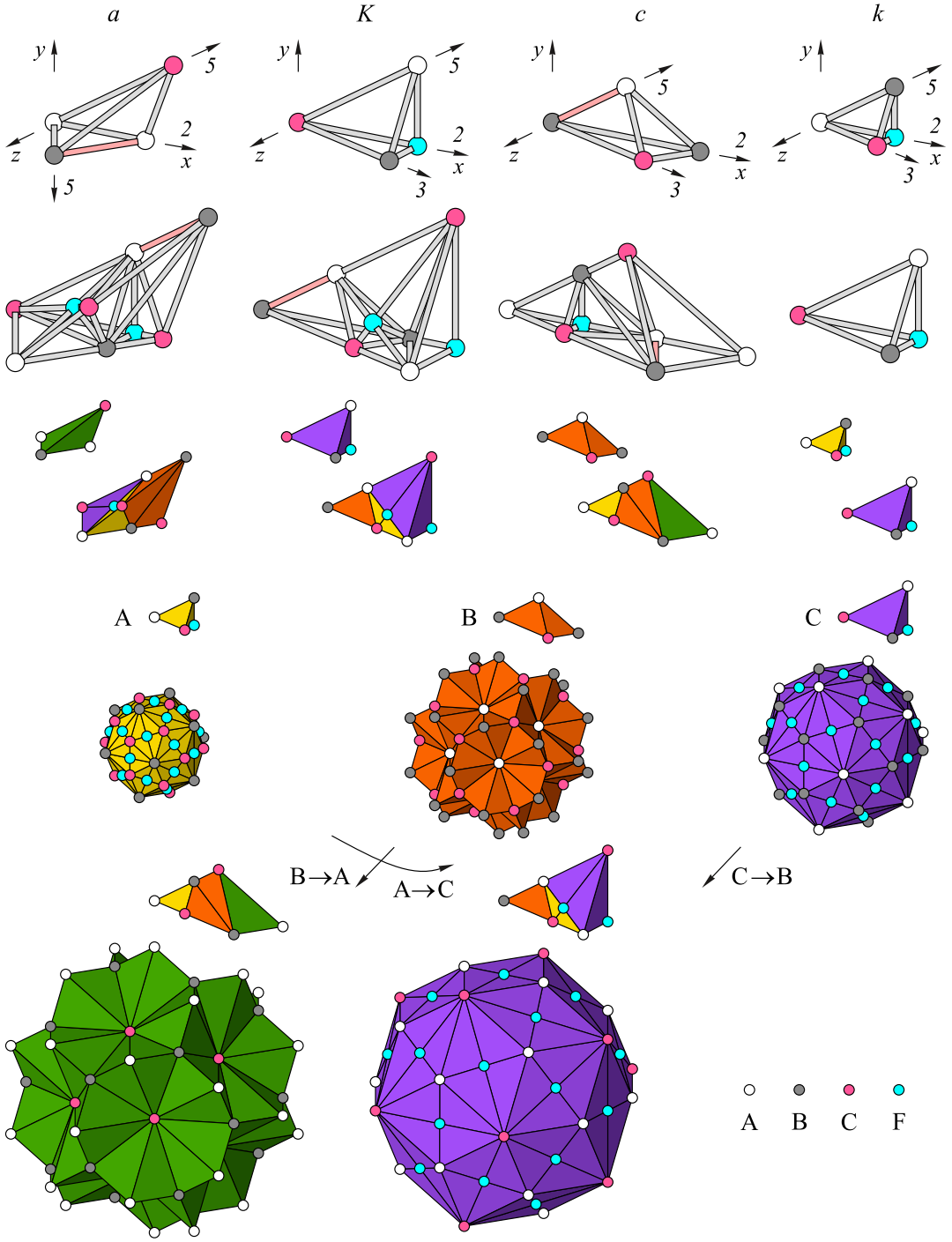


**Figure 2.** Construction of an icosahedral packing of $I$-type based on a tetrahedral $ackK$-tiling. From top to bottom: a basis set of 4 tetrahedra $\{a, c, k, K\}$ in standard orientation and substitution rules in the form of ball-and-stick models; substitution rules in the form of tetrahedron packings; 3 tetrahedra used to initialize the construction procedure of 3 packing variants (centered at nodes A, B, C), symmetric starting configurations made up of them and the result of application of the 1st iteration to them. Nodes of different types are highlighted in colors: A (white), B (black), C (red), F (turquoise).

120 tetrahedra $c$ and 240 tetrahedra $k$, together forming a star of rhombohedra. This transformation is marked with an oblique arrow from C to B in Fig. 2. Further, the packing generation process continues until the desired size is reached.

An icosahedral packing of $F$-type is constructed by us on the basis of the classical Danzer tiling, the tetrahedra of which are reduced by $\tau$ times (Fig. 3). The figure shows 4 tetrahedra of the basis set in the orientations, which we have accepted as the standard, the substitution rules for

**Table 3.** Substitution rules for $F$-type packing

| № $j$ | Type of cell | Position $\mathbf{R}_j$ | Orientation № | $g_j$ |
|---|---|---|---|---|
| | | $a \to \mathrm{infl}(a)$ | | |
| 1 | $b$ | (0, 0, 0) | 1 | 1 |
| 2 | $b$ | (0, 0, 0) | 111 | $m(15)$ |
| 3 | $b$ | (0, 0, 0) | 28 | $3(154)$ |
| 4 | $k$ | $(1+\tau, \tau, 0)$ | 41 | $3^2(237)$ |
| 5 | $k$ | $(1+\tau, \tau, 0)$ | 64 | $\overline{5}(3)$ |
| 6 | $k$ | $(\tau, 0, 1+\tau)$ | 60 | $2(49)$ |
| 7 | $k$ | $(1+\tau, \tau, 0)$ | 104 | $\overline{3}^5(498)$ |
| 8 | $k$ | $(1+\tau, \tau, 0)$ | 20 | $5^3(1)$ |
| 9 | $k$ | $(\tau, 0, 1+\tau)$ | 102 | $\overline{3}^5(387)$ |
| 10 | $c$ | $(1+2\tau, 1+\tau, 0)$ | 54 | $2(56)$ |
| 11 | $c$ | $(1+2\tau, 1+\tau, 0)$ | 77 | $\overline{5}^7(4)$ |
| | | $b \to \mathrm{infl}(b)$ | | |
| 1 | $c$ | (0, 0, 0) | 1 | 1 |
| 2 | $k$ | $(\tau, 1, 0)$ | 76 | $\overline{5}^7(3)$ |
| 3 | $k$ | $(1+2\tau, 0, \tau)$ | 55 | $2(26)$ |
| 4 | $k$ | $(1+\tau, \tau, 0)$ | 38 | $3^2(154)$ |
| 5 | $k$ | $(1+2\tau, 0, \tau)$ | 66 | $\overline{5}(5)$ |
| 6 | $b$ | $(1+2\tau, 1+\tau, 0)$ | 54 | $2(56)$ |
| 7 | $b$ | $(1+2\tau, 1+\tau, 0)$ | 63 | $\overline{5}(2)$ |
| | | $c \to \mathrm{infl}(c)$ | | |
| 1 | $k$ | (0, 0, 0) | 1 | 1 |
| 2 | $k$ | $(2\tau, 0, 0)$ | 113 | $m(12)$ |
| 3 | $c$ | $(1+2\tau, 0, \tau)$ | 55 | $2(26)$ |
| 4 | $c$ | $(1+2\tau, 0, \tau)$ | 66 | $\overline{5}(5)$ |
| 5 | $a$ | $(2+2\tau, 0, 0)$ | 113 | $m(12)$ |
| | | $k \to \mathrm{infl}(k)$ | | |
| 1 | $b$ | (0, 0, 0) | 1 | 1 |
| 2 | $k$ | $(1+\tau, \tau, 0)$ | 41 | $3^2(237)$ |

them, the starting configurations, and the result of applying the 1st iteration. The substitution rules for the Danzer tiling with reduced tetrahedra are given in Table 3.

The Danzer tiling is also characterized by a cyclic change of node types: 3 variants of locally isomorphic patches cyclically transform into each other after each iteration for both tetrahedral tilings.

There is an analogy here with the properties of the Penrose tiling. For it, the inflation factor is $\tau$ whereas the self-similarity factor is $\tau^2$. Two configurations („star“ and „sun“) cyclically transform into each other after each iteration [32]. Most likely, self-similar rhombic tilings with the 7-fold symmetry [33] would have similar property if the problem with the ambiguity of the deflation rules could be solved.

We believe that a similar algorithm, after making minor changes, can be applied to construct almost any tiling based on substitutions (*substitution tilings*) [29], including cyclotomic tilings with higher-symmetry axes [34], self-similar rhombic tilings with 7-fold symmetry and multiple substitution rules for tiles of the same shape [33], tilings with a dense distribution of possible tile orientations similar to the Conway-Radin pinwheel [35,36] and others.

## 3. Enantiomorphism

The general principles of constructing non-centrosymmetric packings were briefly outlined in the previous part [2]. All 120 copies of each of the tetrahedra are equivalent in the group $I_h$. Differently oriented cells and their mirror copies should be considered different in the group $I$. It would be possible to group several tetrahedra of the same type with their mirror copies into asymmetric octahedra [29] and then use them as asymmetric unit cells. There is a simpler solution.

First of all, let us make a clarification. All 3 types of packings are considered within the framework of the proposed theory — $P$, $I$, $F$. Here, the symbol $I$ traditionally denotes the icosahedral analogue of a body-centered cubic lattice. All 3 types can have both a symmetry group $I_h$ and a symmetry group $I$. In this context, the symbol $I$ corresponds to the group of pure rotations of an icosahedron in Schoenflies notation. Where there may be discrepancies, we will add Hermann-Mauguin symbols to the symbols of the symmetry group: 235 ($I$), $m\overline{3}5$.

So, let us start by considering a packing of $I$-type with symmetry 235 (group $I$). Let us take the tetrahedra of the basis set $\{a, c, k, K\}$ and rotate them with all the symmetry elements of the group $I_h$. This will result in 120 orientations each. Half of them can be considered as „right“ while the other half as the „left“ ones. There is no need to choose the cells of other shapes, and there is no need to make changes to the packing algorithm. It is enough to look at the orientation number of a particular cell in the list. If the number is in the range from 61 to 120, then this is a mirrored orientation.

The initial orientation and the orientations obtained from it by using the subgroup of pure rotations $I$ will be considered as the right-oriented ones for tetrahedra $\{c, k, K\}$, the rest will be considered as the left-oriented ones. The exception to the general rule is the tetrahedron $a$, for which the order of determining the right and left orientations must be reversed. Thanks to this choice, a tetrahedron packing will be built according to the „face-to-face“ principle, and the right-oriented tetrahedron in it will always be adjacent to the left-oriented one, regardless of its specific type.

When constructing a non-centrosymmetric packing of $F$-type, the only difference is that the set $\{a, b, c, k\}$ is used instead of the set $\{a, c, k, K\}$. The two right and two left tetrahedra $b$ and $k$ are grouped together and used instead of the corresponding right and left tetrahedra $K$. The general principle that the face of the right tetrahedron always touches the face of the left one is violated only in the case of a shared face of a pair of neighboring tetrahedra $b$ and $k$.

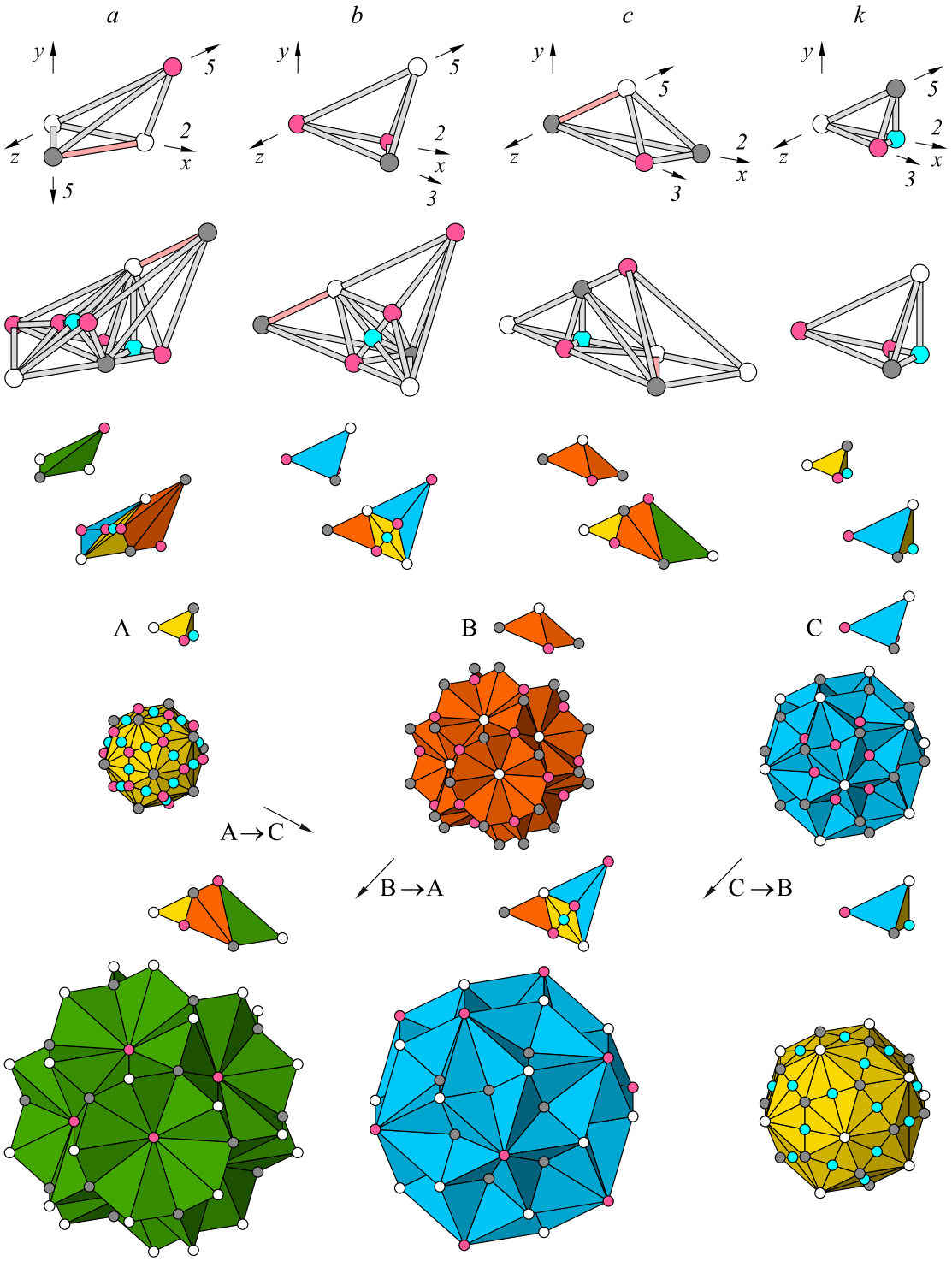


**Figure 3.** Construction of an icosahedral packing of $F$-type based on a tetrahedral $abck$-tiling. From top to bottom: a basis set of tetrahedra $\{a, b, c, k\}$ in standard orientation and substitution rules in the form of ball-and-stick models; substitution rules in the form of tetrahedron packings; 3 tetrahedra used to initialize the construction procedure of 3 packing variants (centered at nodes A, B and C), the symmetric starting configurations made up of them and the result of application of the 1st iteration to them.

The construction of non-centrosymmetric icosahedral packings is explained in Figs. 4, 5.

Fig. 4 shows the right and left Danzer tetrahedra used to construct non-centrosymmetric icosahedral packings. The left orientations are obtained from the right ones using the inversion operation. If we take the set $\{a, b, c, k\}$, which is used to build the packing $F$, and choose the pair of right and left tetrahedra $K$ instead of the corresponding pair of

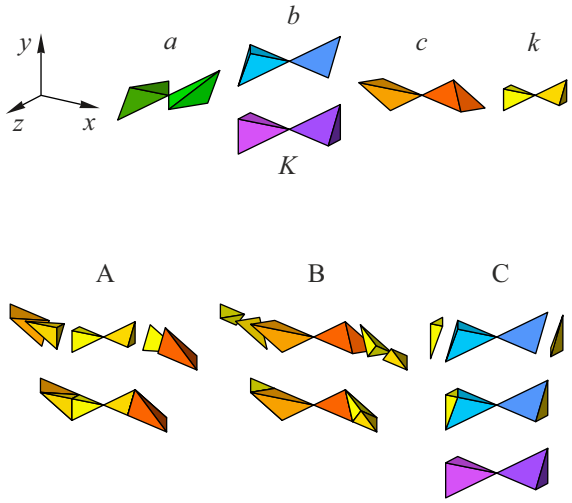


**Figure 4.** Principles of constructing non-centrosymmetric icosahedral packings; at the top — the orientation of the coordinate axes used and the basis sets of right and left Danzer tetrahedra oriented relative to them; at the bottom — tetrahedron configurations used to initialize 3 packing variants (centered at nodes A, B, C). Darker color palettes are used to draw the right tetrahedra in the color version of the drawing presented in the electronic version of the article.

tetrahedra $b$, we obtain a set $\{a, c, k, K\}$ for building the packing $I$.

The right and left tetrahedra in the symmetry group 235 ($I$) are not equivalent. Formally, the basis sets contain twice the number of tetrahedra: $\{\overline{a}, c, k, K, a, \overline{c}, \overline{k}, \overline{K}\}$ for packing of $I$-type generated from a six-dimensional bcc lattice, and $\{\overline{a}, b, c, k, a, \overline{b}, \overline{c}, \overline{k}\}$ for packing of $F$-type generated from a six-dimensional fcc lattice. Here, we used the inversion symbol to denote tetrahedra in the mirrored orientation. However, once again, the procedure for constructing packings for groups $I$ and $I_h$ is no different. Differences for the group $I$ appear only at the next stage, when the method of decorating cells with specific atoms is chosen, depending on whether the cell orientation falls within the range 1−60 or in the range 61−120 (see Table 4 in the Appendix).

Fig. 4 also shows the configurations used to initialize the procedure for constructing 3 packing variants (centered at nodes A, B, and C). The starting configurations are two different stars of rhombohedra (hexecontahedra) and triacontahedron in this case. The analogy with the construction of the Socolar-Steinhardt tiling [22,24] becomes obvious. This allows establishing an exact correspondence between packings of tetrahedra and packings of zonohedra, and, ultimately, between all three types of quasilattices ($P, I, F$).

The construction of a packing of $I$-type with symmetry 235 ($I$) is shown in Fig. 5. The starting configurations are 2 hexecontahedra (variants A and B of the packing $I$), differing in the orientation of the rhombohedra forming them, and a triacontahedron (variant C of the packing $I$). The results of applying 3 consecutive iterations are presented. The sizes of all patches increase by $\tau$ times with each iteration, and the types of all nodes are cyclically interchanged C→B→A→C. As a consequence, 3 locally isomorphic packing variants transform into each other. In particular, 120 tetrahedra $K$ are combined into a triacontahedron (the starting configuration of the packing variant C), it increases by $\tau$ times and becomes a fragment of the packing B, then it increases again and becomes a fragment of the packing A and only after the 3rd iteration it becomes the packing C again.

Packing variants differ by the type of the node at the origin: A, B, C. In Fig. 5, larger and larger patches of 3 different packing variants are arranged in horizontal rows. The starting configurations and the results of applying 3 consecutive iterations to them are arranged in vertical columns. The arrows indicate that, after each iteration, the fragments of packings with nodes of various types in the center not only increase in size, but also cyclically transform into each other.

Let us pay attention to the fundamental differences in the symmetry of the ornaments obtained on different faces and the alternation of the right and left tetrahedra forming the packing.

A triacontahedron enlarged by $\tau^3$ times contains more than 12 000 base tetrahedra oriented in various ways, and the stars of rhombohedra after 3 iterations contain more than 16 000 tetrahedra. It is not difficult to verify this by cubing the tiling composition matrix given in the first part of the work [2].

The construction of a packing of $F$-type is completely similar. The generation of large fragments of the Danzer tiling was reported in the literature [37]. Perhaps the small number of tetrahedra was not sufficient to establish the fundamental properties of icosahedral packings, and their large number complicated the analysis too much.

## 4. Packing of *P*-type

There is a well-established opinion in the literature that the Socolar-Steinhardt tiling into zonohedra is completely equivalent to the Danzer *ABCK*-tiling into tetrahedra (with the correction that equivalence is implied in the sense of their mutual local derivability) [10]. It has also been argued that both of these tilings describe icosahedral analogues of the face-centered cubic lattice [38]. Once again, the packing of zonohedra describes quasicrystals of $P$-type, i.e. analogues of the primitive cubic lattice [1,2].

The substitution rules for the packing of zonohedra were derived by us in Refs. [22,23] almost three decades after its discovery [8]. The formalization of the algorithm for constructing the packing of zonohedra made it possible to establish a number of important features [24,27]. It is sufficient to set the positions and orientations of only 12 polyhedra to derive the deflation scheme of a triacontahedron, but after multiplying them by the symmetry group of the icosahedron, the complete deflation scheme of the

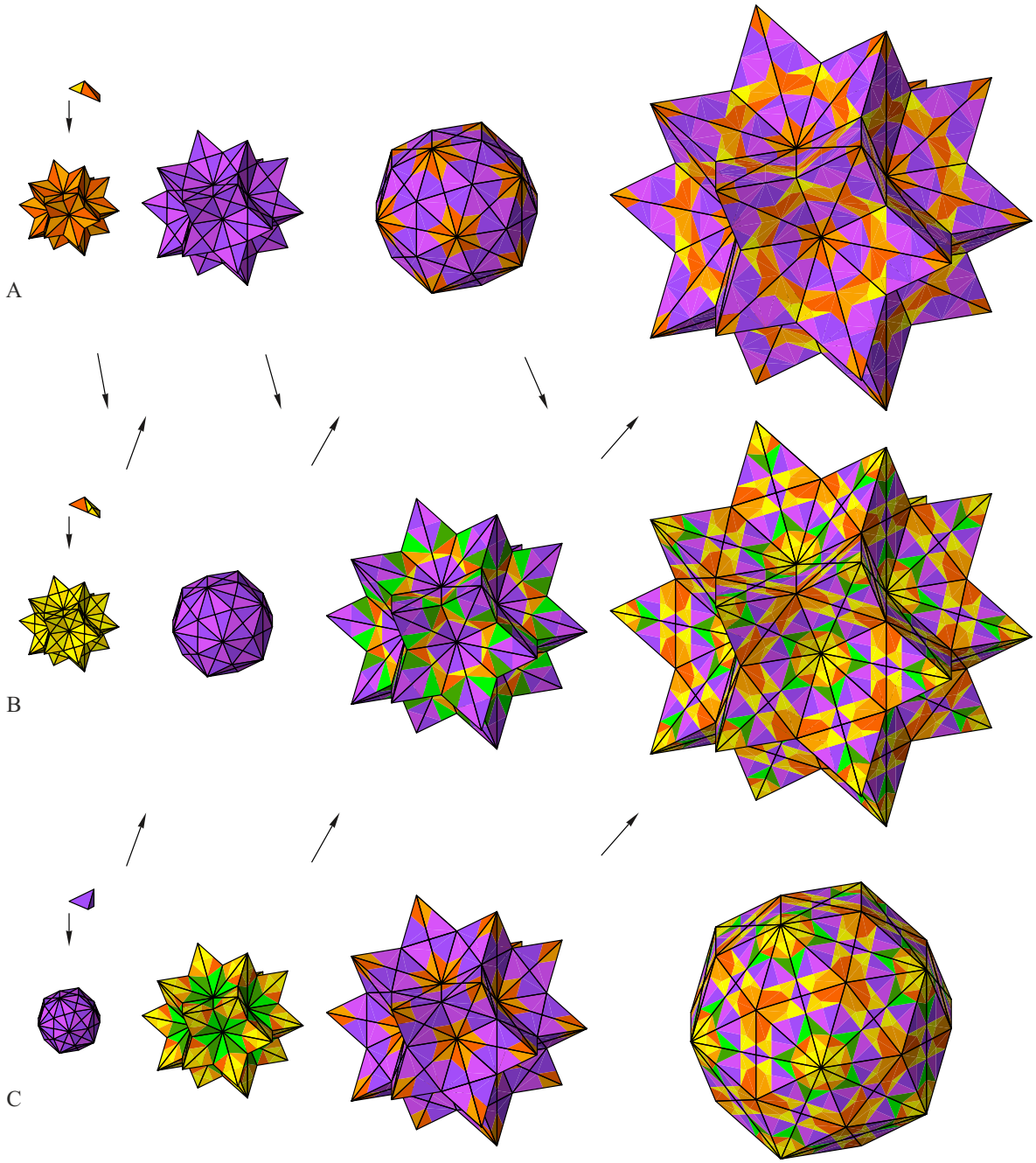


**Figure 5.** Construction of an icosahedral packing of $I$-type with symmetry 235 ($I$). The starting configurations are 2 stars of rhombohedra (A and B) and a triacontahedron (C). The results of applying 3 iterations are presented. The sizes of all configurations increase by $\tau$ times with each iteration, and the types of all nodes are cyclically interchanged C→B→A→C.

triacontahedron will already contain a list of 533 entries. The deflation schemes of the remaining zonohedra are derived from the deflation scheme of the triacontahedron. As a result, the whole list of polyhedra forming substitution rules for all 4 zonohedra occupies several tens of pages.

There is another option — to add the „fictitious“ nodes C, build the $I$-type packing of tetrahedra $\{a, c, k, K\}$, and then remove all the newly introduced type C nodes from the just constructed tiling. Since the centering scheme of the $I$-type only adds new nodes to the primitive cubic $6D$-lattice, but does not change the lattice $Z^6$ itself, their removal is expected to return things to the way they were — to the lattice of $P$-type. We have already noted that the inflation factor for quasicrystals of $P$-type is equal to $\tau^3$. Therefore, our task is to establish a correspondence between the substitution rules for zonohedra and the 3rd iteration of the inflation-deflation algorithm for packing Danzer tetrahedra with the basis set $\{a, c, k, K\}$.

The relationship between the Socolar-Steinhardt tiling into golden zonohedra and tilings based on Danzer tetrahedra is illustrated in Fig. 6. As expected, tetrahedra $\{a, c, k, K\}$ grouped around a common vertex C form zonohedra

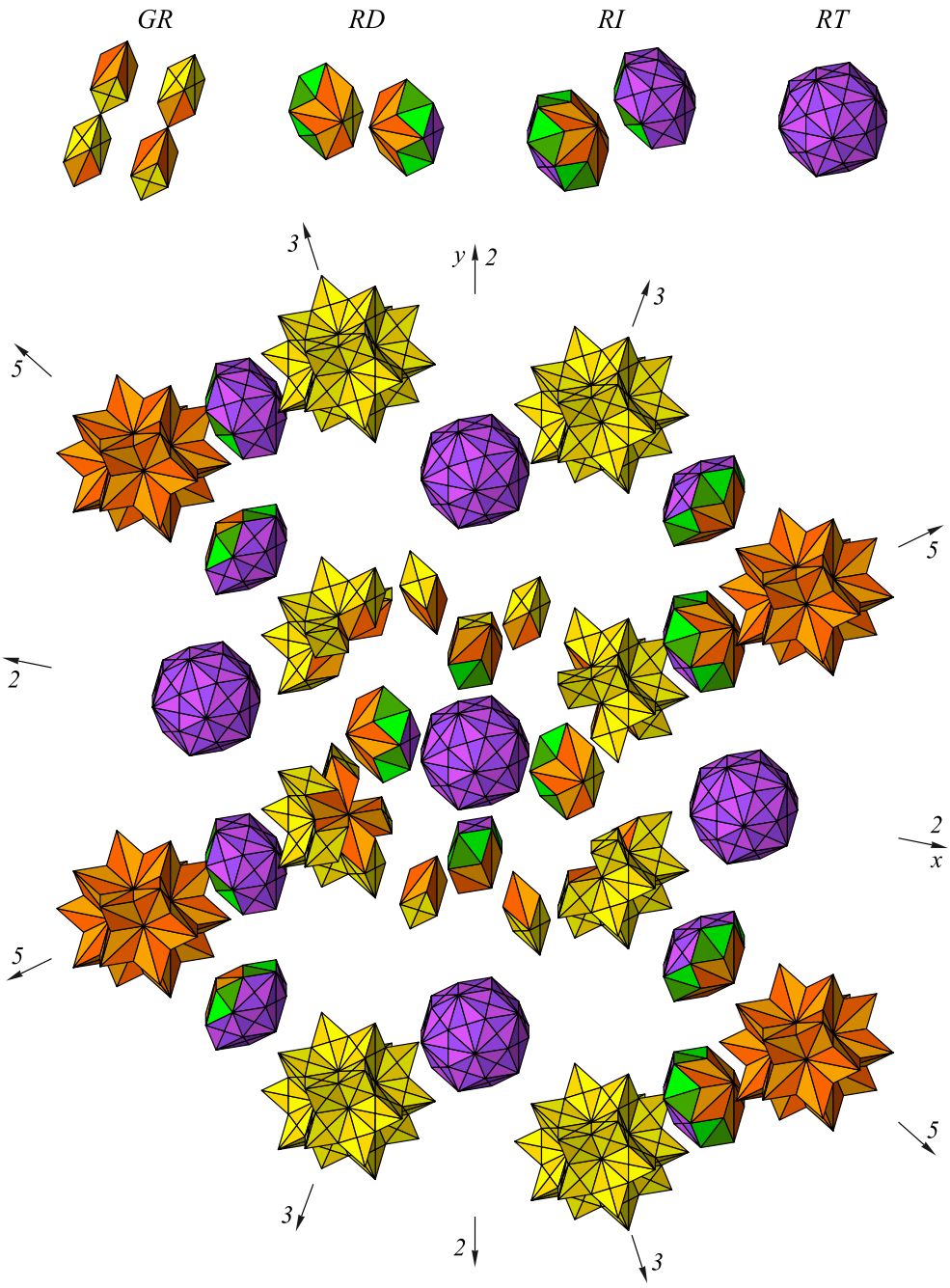


**Figure 6.** The relationship between the Socolar-Steinhardt tiling into golden zonohedra and tilings based on Danzer tetrahedra. Above: tetrahedra $\{a, c, k, K\}$ grouped around a common vertex C form zonohedra $\{GR, RD, RI, RT\}$. In the center: the exact correspondence between the substitution rules for zonohedra and packing of $I$-type based on Danzer tetrahedra. A layer cut perpendicular to the 2-fold axis (packing variant with node C in the center) is shown. Tetrahedra are combined into zonohedra. The spatial arrangement of the zonohedra exactly reproduces the substitution rule for the triacontahedron in the Socolar-Steinhardt tiling. The arrows indicate the 2, 3 and 5-fold symmetry axes and illustrate their location with respect to the coordinate axes $x$ and $y$, the $z$-axis is directed perpendicular to the layer.

$\{GR, RD, RI, RT\}$. An equivalent zonohedron dissection scheme, but for the standard Danzer tiling, was described in Ref. [38]. A careful comparison of the packings allowed establishing an exact correspondence between the substitution rules for zonohedra and packing of $I$-type based on Danzer tetrahedra. Fig. 6 shows the packing layer, cut perpendicular to the 2-fold axis (coinciding with the $z$-axis). This is the variant with node C in the center. If tetrahedra are combined into zonohedra, then their spatial arrangement exactly reproduces the substitution rule for the triacontahedron in the Socolar-Steinhardt tiling.

It should be noted that the approach based on deriving the zonohedral tiling from the tetrahedral one, in addition

to simplifying the packing algorithm, also greatly simplifies the subsequent procedure for populating cells with atoms.

Let us pay attention once again to the alternation of right and left tetrahedra. When constructing zonohedral packing using the set $\{a, c, k, K\}$, the right tetrahedra are always adjacent to the left ones — both when combining them into zonohedra and when combining zonohedra into a global packing. This property imposes additional limitations on the options for decorating cells with atoms, since in this case, in addition to the local symmetry of the zonohedra, the local matching rules between the touching faces should also be taken into account. This property allows using the „plug-and-socket" principle when assembling subunits, especially if, for example, we are faced with the task of constructing full-scale physical models of various icosahedral packings. It becomes possible to build models of complex quasicrystalline packings based on the principle of a children's designer. It is also possible to map the tiling to a bipartite graph and derive useful consequences using graph theory methods.

## 5. Results and discussion

This paper is the second in a series of papers on the theory of the structure of icosahedral quasicrystals. We explained in detail the procedure for deriving three main types of icosahedral tilings by projection from a six-dimensional space and established their exact relationship with three types of icosahedral quasicrystals in our previous work [2]. It has been shown that the Socolar-Steinhardt zonohedral tiling corresponds to a quasilattice of $P$-type. All vertices of zonohedra have as their prototypes the nodes of a primitive cubic $6D$-lattice generated by six unit basis vectors — vector [1 0 0 0 0 0] and equivalent vectors obtained by cyclic permutations of coordinates. The reverse is not true — not all nodes within the projection strip should be taken into account when mapping in $3D$-space to avoid violating icosahedral symmetry. All additional nodes of the quasilattice of $I$-type have as their prototypes the nodes of the cubic $6D$-sublattice shifted by a vector $[\frac{1}{2}\ \frac{1}{2}\ \frac{1}{2}\ \frac{1}{2}\ \frac{1}{2}\ \frac{1}{2}]$. The additional nodes of the quasilattice of $F$-type have as their prototypes the nodes of the sublattices shifted by the vector $[\frac{1}{2}\ \frac{1}{2}\ 0\ 0\ 0\ 0]$ and equivalent shifts. The quasilattices $I$ and $F$ correspond to two tetrahedral Danzer tilings with basis sets $\{a, c, k, K\}$ and $\{a, b, c, k\}$, respectively. Thus, the approach based on the tiling theory does not contradict the methods of higher-dimensional crystallography, but is a natural and integral part of it.

Well-known statements about the supposedly complete mutual equivalence of zonohedral and tetrahedral packings [9,38] may lead an unprepared reader to erroneous conclusions. The concept of mutual derivability in Ref. [39] implies not the true equivalence, but only that the polyhedra of one of the tilings can be dissected into smaller parts, which can then be re-grouped into polyhedra of the second tiling. In this sense, a fcc lattice can indeed be derived from a primitive one, and the result of projecting one of them can be derived from the result of projecting the other. It would be useful to mention the kagome grid as another illustrative counterexample, in which hexagons can be dissected into smaller parts in such a way that the pairs of cut triangles can be combined with pairs of equilateral triangles. This results in a rectangle checkerboard pattern with alternating centered and empty rectangles. A pair of plane grids with fundamentally different symmetries satisfies all the requirements of mutual local derivability, which, however, does not mean at all that they are equivalent.

Let us formulate an important thesis. The iterative algorithm of inflation and deflation underlies the procedure for constructing all the tilings considered in the present paper. As a result, they have all the properties inherent in tilings of this type [29]. Any statements that are valid with respect to the result of the 1st iteration can be extended to a sufficiently large region of finite dimensions and elementarily proved by induction.

Some complications may arise in the case of the so-called „imperfect" substitution rules. The enlarged tiles are still filled with tiles of the original size, but they may not completely cover the corresponding areas, or partially extend beyond their boundaries. Cells located on the boundaries of supercells are generated several times, and the overall boundary of the generated area becomes fractal after several iterations. The problems that arise in this case are easy to solve algorithmically: all the duplicate elements in the list of cells should be deleted after each iteration, as well as cells that go beyond the enlarged area entirely. The Penrose tiling is the most famous example of an inflation tiling with imperfect rules. In the three-dimensional case, the substitution rules for Danzer tetrahedra are perfect, but the rules for zonohedra built up of them are imperfect.

The substitution rules that we derived for the Socolar-Steinhardt tiling [22] were later used to construct sufficiently large representative patches of icosahedral packings by both us and other researchers. At least 3 papers have been featured on the covers of the corresponding issues by the editors of reputable scientific journals [40–42], which can be indirectly considered as a successful verification of the theoretical concepts we use, including by independent researchers. This paper presents the results of applying a similar approach to the analysis of all currently known variants of icosahedral packings.

Now we can formulate the main differences of our theoretical consideration from the widely accepted model of overlapping clusters and the model with two types of rhombohedra. The existence of a characteristic structural motif of two (or more) overlapping triacontahedra was experimentally established in the structures of approximants. In particular, it is characteristic of a large class of intermetallic compounds, differing in the number and type of their constituent components — crystalline 2/1-approximants. Their structures were determined under the assumption of the Fedorov space groups $Pa\overline{3}$ and $Im\overline{3}$ [43].

We would like to remind that the structures of approximants can also be obtained by projection from spaces of higher dimensions. The only difference is that the structures

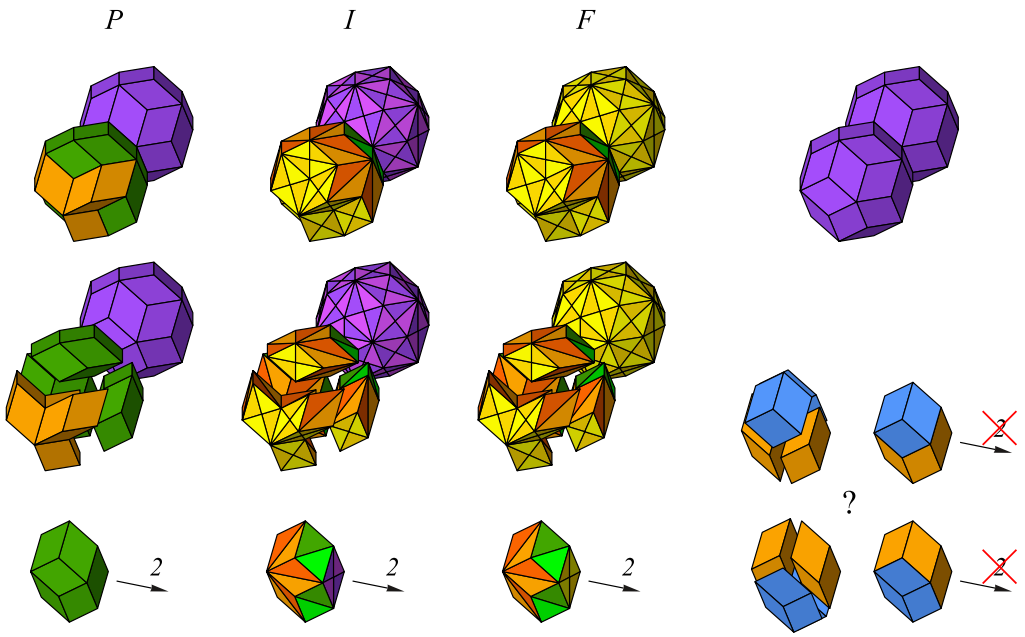


**Figure 7.** Fundamental differences between fragments of 3 types of icosahedral packings ($P$, $I$, $F$) and their corresponding characteristic fragments in the overlapping cluster model and in models based on two types of rhombohedra (prolate and oblate). Above: on the left, a triacontahedron combined with a cluster of three rhombic Bilinski dodecahedra and four prolate rhombohedra, possible ways to implement a characteristic cluster in packings of three types are shown; on the right, two mutually overlapping triacontahedra in the structures of crystalline approximants. Below: illustration of the ambiguity of projection and symmetry breaking when using a basis set of two types of rhombohedra (prolate and oblate) by using the Bilinski dodecahedron as an example; on the left — rhombic dodecahedra in packings of three types, local 2-fold axes pass through the rhombic dodecahedra; on the right — two variants of dissections of the Bilinski dodecahedron into prolate and oblate rhombohedra, both of which lead to the loss of the original symmetry.

of quasicrystals are obtained when projected along irrational directions, and approximants — along rational directions close to them [44–46]. As a result, the approximants are characterized by a similar stoichiometric composition and similar structural motifs, but they are ordinary periodic crystals (with a sufficiently large number of atoms in a unit cell). It should be noted that recently the concept of an approximant has been interpreted in a broader sense [47].

So, overlapping icosahedral clusters were initially found in crystal structures. The model of overlapping triacontahedra perfectly agrees with the periodic structure of crystalline approximants, but poorly agrees with the aperiodic structure of quasicrystals. Its use is based on a completely natural structural analogy, but, as shown below, it leads to a violation of the exact icosahedral symmetry on a larger scale.

Fig. 7 clearly illustrates the incompatibility of structural models widely used in practice with the detailed structure of all three main icosahedral packings. On the one hand, these models are used to fit and refine the structures of real quasicrystals during projection within the framework of a higher-dimensional approach. On the other hand, all three types of icosahedral packings are also derived by projection from a six-dimensional space. The iterative algorithm of inflation and deflation greatly simplifies the procedure for constructing packings compared to the direct projection, but basically this algorithm is a consequence of the inflation symmetry, i.e. the substitutions should not contradict the higher-dimensional approach either.

When comparing the model of overlapping triacontahedra with the corresponding fragments of zonohedral packing (Fig. 7), we conclude that the initial triacontahedron is not adjacent to a second identical triacontahedron overlapping with the first, but to a cluster of three rhombic Bilinski dodecahedra and four prolate rhombohedra. Its shape is similar to that of a triacontahedron, but its internal structure and symmetry are radically different. It does not have icosahedral symmetry. An attempt to identify it with a triacontahedron when fitting a real structure should lead to a decrease in symmetry and the appearance of statistically averaged „false“ positions, which are usually interpreted as mixed or partially occupied positions. Further dissection of zonohedra into Danzer tetrahedra in packings $I$ and $F$ does not fundamentally change anything — the second half of the cluster is not identical to the first.

As already noted, the structure of icosahedral quasicrystals is often considered by many researchers as a tiling into two types of rhombohedra, prolate and oblate (Penrose 3$D$-tiling, tiling into Ammann rhombohedra, Ammann–Kramer–Neri tiling). The fundamental problems that arise with this approach were first pointed out by Socolar and Steinhardt: „It [a triacontahedron] can be resolved into ten prolate and ten oblate rhombohedra in many different ways, but in none of them is the full icosahedral symmetry preserved“ [8]. Later, they attempted to build an Amman tiling by introducing a set of several local matching rules which were used depending on the context [48].

Here is a rather long quote from Steurer's article in „*International Tables*“ — one of the most reputable published by the International Union of Crystallography [3]: „Ten prolate and ten oblate rhombohedra can be packed to form a rhombic triacontahedron. The icosahedral symmetry of this zonohedron is broken by the many possible decompositions into the rhombohedra. Removing one zone of the triacontahedron gives a rhomb-icosahedron consisting of five prolate and five oblate rhombohedra. Again, the singular fivefold axis of the rhomb-icosahedron is broken by the decomposition into rhombohedra. Removing one zone again gives a rhombic dodecahedron consisting of two prolate and two oblate rhombohedra. Removing the last remaining zone leads finally to a single prolate rhombohedron. Using these zonohedra as elementary clusters, a matching rule can be derived for the 3*D* construction of the 3*D* Penrose tiling.“ Surprisingly, but a fact — for decades, models have been used in the structural analysis of quasicrystals that are obviously incompatible with icosahedral symmetry! Conversely, models that accurately reproduce local and global icosahedral symmetry have almost never been used in structural studies.

The ambiguity of the projection procedure and the violation of symmetry in the case of using two types of rhombohedra (prolate and oblate) are explained in Fig. 7, *below* using the Bilinski dodecahedron as an example. The rhombic dodecahedron appears directly as one of the zonohedra of the basis set in the packings of *P*-type. It can be additionally dissected into Danzer tetrahedra of the corresponding basis sets in the packings of *I* and *F*-types. The local 2-fold axes pass through the rhombic dodecahedra. The intrinsic symmetry of the zonohedra is not violated in all three packings we use. There are 2 variants of dissection of the Bilinski dodecahedron into prolate and oblate rhombohedra, which are shown on the right. Both variants lead to the loss of the initial symmetry — both the local symmetry of a particular cell or a cluster of cells and the global icosahedral symmetry of the packing as a whole are violated.

Once again, the dissection of zonohedra into rhombohedra cannot be defined unambiguously. The ambiguity of the projection generates a special type of defects in quasicrystals — phasons [49]. On the contrary, the construction process of all three packings considered by us is completely deterministic. In our opinion, the choice in favor of models with ambiguous subdivision into subcells should be justified by the presence of properties characteristic of such structures. Experiments should show a real decrease of local symmetry and a high probability of strongly correlated effects associated with atomic „jumps“ between neighboring partially occupied positions (if they actually occur), which should most likely be accompanied by local rearrangements at the atomic level and the formation of a secondary domain structure by analogy with ferroelectrics.

We plan to outline the rules for filling the unit cells with specific atoms in the next paper. We suppose that the general and special positions should be defined within the unit cells of quasicrystals similar to the Wyckoff positions in the unit cells of conventional crystals. This will make it possible to move from considering packings of polyhedra to generating quasiperiodic structures with the desired spatial arrangement of atoms and to studying their possible physical properties. An important part of this approach is the averaging over the volume based on substitutions and adopted to handle the lists of cells [24].

## Conclusion

We consider icosahedral quasicrystals as packings of unit cells. All possible variants of self-similar icosahedral packings are analyzed within the framework of a single approach. There are 3 types of icosahedral quasicrystals ($P$, $I$, $F$) — analogues of primitive, body-centered and face-centered cubic lattices, respectively. Centrosymmetric and non-centrosymmetric structures are possible for each type, for each of which there are 3 locally isomorphic variants.

We concluded that a packing of *P*-type corresponds to Socolar-Steinhardt tiling into zonohedra, and packings of *I* and *F*-types correspond to two different tilings based on Danzer tetrahedra. Despite the fact that each of these three tilings uses its own basis set of unit cells and its own substitution rules, they are completely mutually consistent. The quasilattice *I* is obtained by adding additional nodes to the quasilattice *P*, and the quasilattice *F* is obtained by adding nodes to the quasilattice *I*. The reverse is also true: some tetrahedra of the packing *F* can be grouped in a certain way resulting in the packing *I*; in turn, the tetrahedra of the packing *I* can be grouped into zonohedra resulting in the packing *P*.

Substitution rules for tilings of *I* and *F*-types into Danzer tetrahedra have been fully formalized. They are represented as lists of cells, each of which is specified by its type, position, and orientation. It is shown how to construct a zonohedral packing of *P*-type from a Danzer tetrahedral packing of *I*-type.

Quasicrystals of all 3 types may or may not have an inversion center (symmetry groups $m\bar{3}5$ or 235). An example of constructing a non-centrosymmetric packing of *I*-type is presented.

For each type of packing, 3 locally isomorphic variants are possible depending on the type o the node at the origin (A, B, C). They cyclically transform into each other after each iteration C→B→A→C when constructing icosahedral packings based on Danzer tetrahedra. The consequence of this is that the structures of characteristic clusters centered at different nodes are interdependent. One and the same structural motifs repeatedly appears in all three clusters on an enlarged scale (in the ratio of $\tau : 1$).

Any type of icosahedral packing can be generated from a single tetrahedron (including the packing of zonohedra, since it can be obtained from tetrahedral packing by combining tetrahedra).

### Acknowledgments

The authors would like to thank S.V. Kozyrev and V.A. Moshnikov for useful discussions.

### Funding

This study was supported by the Russian Science Foundation (grant No. 23-23-00392, https://rscf.ru/project/23-23-00392/

### Conflict of interest

The authors declare that they have no conflict of interest.

## References

[1] A.E. Madison. Tech. Phys. Lett., **50** (10), 13 (2024).
[2] A.E. Madison, P.A. Madison. Tech. Phys., **69**, 1967 (2024).
[3] W. Steurer, T. Haibach. In: *International Tables for Crystallography Volume B: Reciprocal Space*, ed. by U. Shmueli (Springer, Dordrecht, 2006), v. B, Ch. 4.6, p. 486. DOI: 10.1107/97809553602060000568
[4] W. Steurer, S. Deloudi. *Crystallography of quasicrystals. Concepts, methods and structures* (Springer, Berlin–Heidelberg, 2009), DOI: 10.1007/978-3-642-01899-2
[5] S. Hyde, S. Andersson, K. Larsson, Z. Blum, T. Landh, S. Lidin, B.W. Ninham. *The language of shape: The role of curvature in condensed matter physics, chemistry, and biology* (Elsevier, Amsterdam, 1997), DOI: 10.1016/B978-0-444-81538-5.X5000-X
[6] M. Baake, U. Grimm. Acta Cryst. A, **76**, 559 (2020). DOI: 10.1107/S2053273320007421
[7] M. Senechal. Proc. Steklov Inst. Math., **288**, 259 (2015). DOI: 10.1134/S0081543815010204
[8] J.E.S. Socolar, P.J. Steinhardt. Phys. Rev. B, **34**, 617 (1986). DOI: 10.1103/PhysRevB.34.617
[9] L. Danzer. Discrete Math., **76**, 1 (1989). DOI: 10.1016/0012-365X(89)90282-3
[10] L. Danzer, Z. Papadopolos, A. Talis. Int. J. Mod. Phys. B, **7**, 1379 (1993). DOI: 10.1142/S0217979293002389
[11] P. Kramer, R. Neri. Acta Cryst. A, **40**, 580 (1984). DOI: 10.1107/S0108767384001203
[12] K. Kato, T. Ninomiya. J. Alloys Compd., **342**, 206 (2002). DOI: 10.1016/S0925-8388(02)00180-9
[13] A. Yamamoto, H. Takakura, A.P. Tsai. Phys. Rev. B, **68**, 094201 (2003). DOI: 10.1103/PhysRevB.68.094201
[14] H. Takakura, C. Pay Gómez, A. Yamamoto, M. de Boissieu, A.P. Tsai. Nature Mater., **6**, 58 (2007). DOI: 10.1038/nmat1799
[15] T. Yamada, H. Takakura, H. Euchner, C. Pay Gómez, A. Bosak, P. Fertey, M. de Boissieu. IUCrJ, **3**, 247 (2016). DOI: 10.1107/S2052252516007041
[16] I. Buganski, J. Wolny, H. Takakura. Acta Cryst. A, **76**, 180 (2020). DOI: 10.1107/S2053273319017339
[17] I. Buganski, R. Strzalka, J. Wolny. Acta Cryst. B, **80**, 84 (2024). DOI: 10.1107/S2052520624000763
[18] L.S. Levitov, J. Rhyner. JETP Lett., **47** (12), 760 (1988). http://jetpletters.ru/ps/1099/article_16620.pdf
[19] L.S. Levitov, J. Rhyner. J. Phys. France, **49**, 1835 (1988). DOI: 10.1051/jphys:0198800490110183500
[20] P. Kramer, Z. Papadopolos, D. Zeidler. In: *Symmetries in science V*, ed. by B. Gruber, L.C. Biedenharn, H.D. Doebner (Springer, Boston, 1991), p. 395. DOI: 10.1007/978-1-4615-3696-3_19
[21] P. Kramer, Z. Papadopolos, M. Schlottmann, D. Zeidler. J. Phys. A: Math. Gen., **27**, 4505 (1994). DOI: 10.1088/0305-4470/27/13/024
[22] A.E. Madison. RSC Adv., **5**, 5745 (2015). DOI: 10.1039/C4RA09524C
[23] A.E. Madison. RSC Adv., **5**, 79279 (2015). DOI: 10.1039/C5RA13874D
[24] A.E. Madison, P.A. Madison, V.A. Moshnikov. Tech. Phys., **69**, 528 (2024).
[25] D.A. Rabson, N.D. Mermin, D.S. Rokhsar, D.C. Wright. Rev. Mod. Phys., **63**, 699 (1991). DOI: 10.1103/RevModPhys.63.699
[26] D.B. Litvin. Acta Cryst. A, **47**, 70 (1991). DOI: 10.1107/S0108767390010054
[27] A.E. Madison, P.A. Madison. Struct. Chem., **31**, 485 (2020). DOI: 10.1007/s11224-019-01430-w
[28] J.H. Conway, N.J.A. Sloane. *Sphere packings, lattices and groups*, 3rd ed. (Springer, NY., 1999), DOI: 10.1007/978-1-4757-6568-7
[29] M. Baake, U. Grimm. *Aperiodic order*. V. 1: *A mathematical invitation* (Cambridge Univ. Press, Cambridge, 2013), DOI: 10.1017/CBO9781139025256
[30] A. Al-Siyabi, N. Ozdes Koca, M. Koca. Symmetry, **12**, 1983 (2020). DOI: 10.3390/sym12121983
[31] L.S. Levitov. EPL, **6**, 517 (1988). DOI: 10.1209/0295-5075/6/6/008
[32] A.E. Madison. Struct. Chem., **26**, 923 (2015). DOI: /10.1007/s11224-014-0559-3
[33] A.E. Madison. Struct. Chem., **29**, 645 (2018). DOI: 10.1007/s11224-018-1083-7
[34] S. Pautze. Symmetry, **9**, 19 (2017). DOI: 10.3390/sym9020019
[35] J.H. Conway, C. Radin. Invent. Math., **132**, 179 (1998). DOI: 10.1007/s002220050221
[36] D. Frettlöh, A.L.D. Say-awen, M.L.A.N. De Las Peñas. Indag. Math., **28**, 120 (2017). DOI: 10.1016/j.indag.2016.11.009
[37] K. Shea. In: *Design Computing and Cognition '04*, ed. by J.S. Gero (Springer, Dordrecht, 2004), p. 137. DOI: 10.1007/978-1-4020-2393-4_8
[38] J. Roth. J. Phys. A: Math. Gen., **26**, 1455 (1993). DOI: 10.1088/0305-4470/26/7/008
[39] M. Baake, M. Schlottmann, P.D. Jarvis. J. Phys. A: Math. Gen., **24**, 4637 (1991). DOI: 10.1088/0305-4470/24/19/025
[40] A.E. Madison, P.A. Madison. Proc. Roy. Soc. A, **475**, 20180667 (2019). DOI: 10.1098/rspa.2018.0667
[41] S.-Y. Jeon, H. Kwon, K. Hur. Nat. Phys., **13**, 363 (2017). DOI: 10.1038/nphys4002
[42] L. Casas. J. Appl. Cryst., **53**, 1583 (2020). DOI: 10.1107/S1600576720011772
[43] T. Yamada, N. Fujita, F. Labib. Acta Cryst. B, **77**, 638 (2021). DOI: 10.1107/S2052520621006715
[44] V.E. Dmitrienko. Acta Cryst. A, **50**, 515 (1994). DOI: 10.1107/S0108767393013960
[45] V.E. Dmitrienko, V.A. Chizhikov. Crystallogr. Rep., **51**, 552 (2006). DOI: 10.1134/S106377450604002X
[46] S. Lidin. In: *Handbook of solid state chemistry*, ed. by R. Dronskowski, S. Kikkawa, A. Stein (Wiley-VCH, Weinheim, 2017), p. 73. DOI: 10.1002/9783527691036.hsscvol1002
[47] T. Matsubara, A. Koga, A. Takano, Y. Matsushita, T. Dotera. Nat. Commun., **15**, 5742 (2024). DOI: 10.1038/s41467-024-49843-4
[48] C.T. Hann, J.E.S. Socolar, P.J. Steinhardt. Phys. Rev. B, **94**, 014113 (2016). DOI: 10.1103/PhysRevB.94.014113
[49] M. de Boissieu. Chem. Soc. Rev., **41**, 6778 (2012). DOI: 10.1039/C2CS35212E

*Translated by A.Akhtayamov*

## Appendix

A list of symmetry elements of the groups $I$ (the first 60 elements) and $I_h$ (all 120 elements) is provided in Table 4 in the order used in the formalization of substitution rules. The elements are distributed among conjugacy classes. The crystallographic designations of the symmetry elements are used with additional clarifying information in parentheses. The numbers in parentheses for the 2, 3 and 5-fold axes indicate specific edges, faces and vertices through which these axes pass, and for the mirror planes they indicate one of the pairs of vertices that transform into each other by reflection. The following columns of the table show the cyclic permutations of the icosahedron vertices corresponding to the symmetry elements for the numbering order adopted in the article, and the rotation matrix in the chosen coordinate system. The following abbreviations are used: $u = (\sqrt{5}+1)/4 = \tau/2$, $v = (\sqrt{5}-1)/4 = \tau^{-1}/2$, where $\tau = (1+\sqrt{5})/2$ is the golden ratio.

Rotation matrices are obtained by standard methods of the group theory and representation theory. The entire set of matrices forms the coordinate representation of the group $I_h$. As usual, the identity element corresponds to a unit matrix, and all matrices are orthogonal, therefore, for any symmetry element, the determinant of the matrix is equal to $\pm 1$. The first 60 elements are the pure (proper) rotations. The determinant is equal to 1 for them. The remaining 60 elements are improper rotations (inversion, rotoinversions or rotoreflections, and mirror planes). The determinant is equal to $-1$ for them. When implementing the packing algorithm, it is not necessary to perform the routine matrix multiplication, it is just enough to use the group multiplication table, the entries of which give the result of the multiplication of elements. The rotation matrices in their explicit form are needed to calculate the coordinates of the atoms in the cells.

**Table 4.** Symmetry elements of groups $I$ and $I_h$

| № | Symmetry element | | Cyclic permutation | Rotation matrix |
|---|---|---|---|---|
| 1 | $E$ | 1 | (1)(2)(3)(4)(5)(6)(7)(8)(9)(10)(11)(12) | $\begin{pmatrix} 1 & 0 & 0 \\ 0 & 1 & 0 \\ 0 & 0 & 1 \end{pmatrix}$ |
| 2 | $C_5(1)$ | 5(1) | (1)(2 6 5 4 3)(7 11 10 9 8)(12) | $\begin{pmatrix} 1/2 & -u & v \\ u & v & -1/2 \\ v & 1/2 & u \end{pmatrix}$ |
| 3 | $C_5(2)$ | 5(2) | (1 3 7 11 6)(2)(4 8 12 10 5)(9) | $\begin{pmatrix} 1/2 & -u & -v \\ u & v & 1/2 \\ -v & -1/2 & u \end{pmatrix}$ |
| 4 | $C_5(3)$ | 5(3) | (1 4 8 7 2)(3)(5 9 12 11 6)(10) | $\begin{pmatrix} v & -1/2 & u \\ 1/2 & u & v \\ -u & v & 1/2 \end{pmatrix}$ |
| 5 | $C_5(4)$ | 5(4) | (1 5 9 8 3)(2 6 10 12 7)(4)(11) | $\begin{pmatrix} u & v & 1/2 \\ v & 1/2 & -u \\ -1/2 & u & v \end{pmatrix}$ |
| 6 | $C_5(5)$ | 5(5) | (1 6 10 9 4)(2 11 12 8 3)(5)(7) | $\begin{pmatrix} u & -v & -1/2 \\ -v & 1/2 & -u \\ 1/2 & u & v \end{pmatrix}$ |
| 7 | $C_5(6)$ | 5(6) | (1 2 11 10 5)(3 7 12 9 4)(6)(8) | $\begin{pmatrix} v & -1/2 & -u \\ 1/2 & u & -v \\ u & -v & 1/2 \end{pmatrix}$ |
| 8 | $C_5^4(1)$ | $5^4(1)$ | (1)(2 3 4 5 6)(7 8 9 10 11)(12) | $\begin{pmatrix} 1/2 & u & v \\ -u & v & 1/2 \\ v & -1/2 & u \end{pmatrix}$ |
| 9 | $C_5^4(2)$ | $5^4(2)$ | (1 6 11 7 3)(2)(4 5 10 12 8)(9) | $\begin{pmatrix} 1/2 & u & -v \\ -u & v & -1/2 \\ -v & 1/2 & u \end{pmatrix}$ |
| 10 | $C_5^4(3)$ | $5^4(3)$ | (1 2 7 8 4)(3)(5 6 11 12 9)(10) | $\begin{pmatrix} v & 1/2 & -u \\ -1/2 & u & v \\ u & v & 1/2 \end{pmatrix}$ |
| 11 | $C_5^4(4)$ | $5^4(4)$ | (1 3 8 9 5)(2 7 12 10 6)(4)(11) | $\begin{pmatrix} u & v & -1/2 \\ v & 1/2 & u \\ 1/2 & -u & v \end{pmatrix}$ |
| 12 | $C_5^4(5)$ | $5^4(5)$ | (1 4 9 10 6)(2 3 8 12 11)(5)(7) | $\begin{pmatrix} u & -v & 1/2 \\ -v & 1/2 & u \\ -1/2 & -u & v \end{pmatrix}$ |

**Table 4** (*continued*).

| № | Symmetry element | | Cyclic permutation | Rotation matrix |
|---|---|---|---|---|
| 13 | $C_5^4(6)$ | $5^4(6)$ | (1 5 10 11 2)(3 4 9 12 7)(6)(8) | $\begin{pmatrix} v & 1/2 & u \\ -1/2 & u & -v \\ -u & -v & 1/2 \end{pmatrix}$ |
| 14 | $C_5^2(1)$ | $5^2(1)$ | (1)(2 5 3 6 4)(7 10 8 11 9)(12) | $\begin{pmatrix} -v & -1/2 & u \\ 1/2 & -u & -v \\ u & v & 1/2 \end{pmatrix}$ |
| 15 | $C_5^2(2)$ | $5^2(2)$ | (1 7 6 3 11)(2)(4 12 5 8 10)(9) | $\begin{pmatrix} -v & -1/2 & -u \\ 1/2 & -u & v \\ -u & -v & 1/2 \end{pmatrix}$ |
| 16 | $C_5^2(3)$ | $5^2(3)$ | (1 8 2 4 7)(3)(5 12 6 9 11)(10) | $\begin{pmatrix} -u & -v & 1/2 \\ v & 1/2 & u \\ -1/2 & u & -v \end{pmatrix}$ |
| 17 | $C_5^2(4)$ | $5^2(4)$ | (1 9 3 5 8)(2 10 7 6 12)(4)(11) | $\begin{pmatrix} 1/2 & u & v \\ u & -v & -1/2 \\ -v & 1/2 & -u \end{pmatrix}$ |
| 18 | $C_5^2(5)$ | $5^2(5)$ | (1 10 4 6 9)(2 12 3 11 8)(5)(7) | $\begin{pmatrix} 1/2 & -u & -v \\ -u & -v & -1/2 \\ v & 1/2 & -u \end{pmatrix}$ |
| 19 | $C_5^2(6)$ | $5^2(6)$ | (1 11 5 2 10)(3 12 4 7 9)(6)(8) | $\begin{pmatrix} -u & -v & -1/2 \\ v & 1/2 & -u \\ 1/2 & -u & -v \end{pmatrix}$ |
| 20 | $C_5^3(1)$ | $5^3(1)$ | (1)(2 4 6 3 5)(7 9 11 8 10)(12) | $\begin{pmatrix} -v & 1/2 & u \\ -1/2 & -u & v \\ u & -v & 1/2 \end{pmatrix}$ |
| 21 | $C_5^3(2)$ | $5^3(2)$ | (1 11 3 6 7)(2)(4 10 8 5 12)(9) | $\begin{pmatrix} -v & 1/2 & -u \\ -1/2 & -u & -v \\ -u & v & 1/2 \end{pmatrix}$ |
| 22 | $C_5^3(3)$ | $5^3(3)$ | (1 7 4 2 8)(3)(5 11 9 6 12)(10) | $\begin{pmatrix} -u & v & -1/2 \\ -v & 1/2 & u \\ 1/2 & u & -v \end{pmatrix}$ |
| 23 | $C_5^3(4)$ | $5^3(4)$ | (1 8 5 3 9)(2 12 6 7 10)(4)(11) | $\begin{pmatrix} 1/2 & u & -v \\ u & -v & 1/2 \\ v & -1/2 & -u \end{pmatrix}$ |
| 24 | $C_5^3(5)$ | $5^3(5)$ | (1 9 6 4 10)(2 8 11 3 12)(5)(7) | $\begin{pmatrix} 1/2 & -u & v \\ -u & -v & 1/2 \\ -v & -1/2 & -u \end{pmatrix}$ |
| 25 | $C_5^3(6)$ | $5^3(6)$ | (1 10 2 5 11)(3 9 7 4 12)(6)(8) | $\begin{pmatrix} -u & v & 1/2 \\ -v & 1/2 & -u \\ -1/2 & -u & -v \end{pmatrix}$ |
| 26 | $C_3(132)$ | 3(132) | (1 3 2)(4 7 6)(5 8 11)(9 12 10) | $\begin{pmatrix} -1/2 & -u & v \\ u & -v & 1/2 \\ -v & 1/2 & u \end{pmatrix}$ |
| 27 | $C_3(143)$ | 3(143) | (1 4 3)(2 5 8)(6 9 7)(10 12 11) | $\begin{pmatrix} 0 & 0 & 1 \\ 1 & 0 & 0 \\ 0 & 1 & 0 \end{pmatrix}$ |
| 28 | $C_3(154)$ | 3(154) | (1 5 4)(2 10 8)(3 6 9)(7 11 12) | $\begin{pmatrix} u & -v & 1/2 \\ v & -1/2 & -u \\ 1/2 & u & -v \end{pmatrix}$ |
| 29 | $C_3(165)$ | 3(165) | (1 6 5)(2 10 4)(3 11 9)(7 12 8) | $\begin{pmatrix} 0 & -1 & 0 \\ 0 & 0 & -1 \\ 1 & 0 & 0 \end{pmatrix}$ |
| 30 | $C_3(126)$ | 3(126) | (1 2 6)(3 11 5)(4 7 10)(8 12 9) | $\begin{pmatrix} -1/2 & -u & -v \\ u & -v & -1/2 \\ v & -1/2 & u \end{pmatrix}$ |
| 31 | $C_3(237)$ | 3(237) | (1 8 11)(2 3 7)(4 12 6)(5 9 10) | $\begin{pmatrix} 0 & -1 & 0 \\ 0 & 0 & 1 \\ -1 & 0 & 0 \end{pmatrix}$ |
| 32 | $C_3(387)$ | 3(387) | (1 9 11)(2 4 12)(3 8 7)(5 10 6) | $\begin{pmatrix} -v & -1/2 & u \\ -1/2 & u & v \\ -u & -v & -1/2 \end{pmatrix}$ |

**Table 4** (*continued*).

| № | Symmetry element | | Cyclic permutation | Rotation matrix |
|---|---|---|---|---|
| 33 | $C_3(348)$ | $3(348)$ | (1 9 7)(2 5 12)(3 4 8)(6 10 11) | $\begin{pmatrix} -v & 1/2 & u \\ 1/2 & u & -v \\ -u & v & -1/2 \end{pmatrix}$ |
| 34 | $C_3(498)$ | $3(498)$ | (1 10 7)(2 6 11)(3 5 12)(4 9 8) | $\begin{pmatrix} 0 & 1 & 0 \\ 0 & 0 & -1 \\ -1 & 0 & 0 \end{pmatrix}$ |
| 35 | $C_3(459)$ | $3(459)$ | (1 10 8)(2 11 7)(3 6 12)(4 5 9) | $\begin{pmatrix} u & v & -1/2 \\ -v & -1/2 & -u \\ -1/2 & u & -v \end{pmatrix}$ |
| 36 | $C_3^2(132)$ | $3^2(132)$ | (1 2 3)(4 6 7)(5 11 8)(9 10 12) | $\begin{pmatrix} -1/2 & u & -v \\ -u & -v & 1/2 \\ v & 1/2 & u \end{pmatrix}$ |
| 37 | $C_3^2(143)$ | $3^2(143)$ | (1 3 4)(2 8 5)(6 7 9)(10 11 12) | $\begin{pmatrix} 0 & 1 & 0 \\ 0 & 0 & 1 \\ 1 & 0 & 0 \end{pmatrix}$ |
| 38 | $C_3^2(154)$ | $3^2(154)$ | (1 4 5)(2 8 10)(3 9 6)(7 12 11) | $\begin{pmatrix} u & v & 1/2 \\ -v & -1/2 & u \\ 1/2 & -u & -v \end{pmatrix}$ |
| 39 | $C_3^2(165)$ | $3^2(165)$ | (1 5 6)(2 4 10)(3 9 11)(7 8 12) | $\begin{pmatrix} 0 & 0 & 1 \\ -1 & 0 & 0 \\ 0 & -1 & 0 \end{pmatrix}$ |
| 40 | $C_3^2(126)$ | $3^2(126)$ | (1 6 2)(3 5 11)(4 10 7)(8 9 12) | $\begin{pmatrix} -1/2 & u & v \\ -u & -v & -1/2 \\ -v & -1/2 & u \end{pmatrix}$ |
| 41 | $C_3^2(237)$ | $3^2(237)$ | (1 11 8)(2 7 3)(4 6 12)(5 10 9) | $\begin{pmatrix} 0 & 0 & -1 \\ -1 & 0 & 0 \\ 0 & 1 & 0 \end{pmatrix}$ |
| 42 | $C_3^2(387)$ | $3^2(387)$ | (1 11 9)(2 12 4)(3 7 8)(5 6 10) | $\begin{pmatrix} -v & -1/2 & -u \\ -1/2 & u & -v \\ u & v & -1/2 \end{pmatrix}$ |
| 43 | $C_3^2(348)$ | $3^2(348)$ | (1 7 9)(2 12 5)(3 8 4)(6 11 10) | $\begin{pmatrix} -v & 1/2 & -u \\ 1/2 & u & v \\ u & -v & -1/2 \end{pmatrix}$ |
| 44 | $C_3^2(498)$ | $3^2(498)$ | (1 7 10)(2 11 6)(3 12 5)(4 8 9) | $\begin{pmatrix} 0 & 0 & -1 \\ 1 & 0 & 0 \\ 0 & -1 & 0 \end{pmatrix}$ |
| 45 | $C_3^2(459)$ | $3^2(459)$ | (1 8 10)(2 7 11)(3 12 6)(4 9 5) | $\begin{pmatrix} u & -v & -1/2 \\ v & -1/2 & u \\ -1/2 & -u & -v \end{pmatrix}$ |
| 46 | $C_2(12)$ | $2(12)$ | (1 2)(3 6)(4 11)(5 7)(8 10)(9 12) | $\begin{pmatrix} -1 & 0 & 0 \\ 0 & -1 & 0 \\ 0 & 0 & 1 \end{pmatrix}$ |
| 47 | $C_2(13)$ | $2(13)$ | (1 3)(2 4)(5 7)(6 8)(9 11)(10 12) | $\begin{pmatrix} -u & v & 1/2 \\ v & -1/2 & u \\ 1/2 & u & v \end{pmatrix}$ |
| 48 | $C_2(14)$ | $2(14)$ | (1 4)(2 9)(3 5)(6 8)(7 10)(11 12) | $\begin{pmatrix} v & 1/2 & u \\ 1/2 & -u & v \\ u & v & -1/2 \end{pmatrix}$ |
| 49 | $C_2(15)$ | $2(15)$ | (1 5)(2 9)(3 10)(4 6)(7 12)(8 11) | $\begin{pmatrix} v & -1/2 & u \\ -1/2 & -u & -v \\ u & -v & -1/2 \end{pmatrix}$ |
| 50 | $C_2(16)$ | $2(16)$ | (1 6)(2 5)(3 10)(4 11)(7 9)(8 12) | $\begin{pmatrix} -u & -v & 1/2 \\ -v & -1/2 & -u \\ 1/2 & -u & v \end{pmatrix}$ |
| 51 | $C_2(23)$ | $2(23)$ | (1 7)(2 3)(4 11)(5 12)(6 8)(9 10) | $\begin{pmatrix} -u & -v & -1/2 \\ -v & -1/2 & u \\ -1/2 & u & v \end{pmatrix}$ |
| 52 | $C_2(34)$ | $2(34)$ | (1 8)(2 9)(3 4)(5 7)(6 12)(10 11) | $\begin{pmatrix} -1/2 & u & v \\ u & v & 1/2 \\ v & 1/2 & -u \end{pmatrix}$ |
| 53 | $C_2(45)$ | $2(45)$ | (1 9)(2 12)(3 10)(4 5)(6 8)(7 11) | $\begin{pmatrix} 1 & 0 & 0 \\ 0 & -1 & 0 \\ 0 & 0 & -1 \end{pmatrix}$ |

**Table 4** (*continued*).

| № | Symmetry element | | Cyclic permutation | Rotation matrix |
|---|---|---|---|---|
| 54 | $C_2(56)$ | 2(56) | (1 10)(2 9)(3 12)(4 11)(5 6)(7 8) | $\begin{pmatrix} -1/2 & -u & v \\ -u & v & -1/2 \\ v & -1/2 & -u \end{pmatrix}$ |
| 55 | $C_2(26)$ | 2(26) | (1 11)(2 6)(3 10)(4 12)(5 7)(8 9) | $\begin{pmatrix} -u & v & -1/2 \\ v & -1/2 & -u \\ -1/2 & -u & v \end{pmatrix}$ |
| 56 | $C_2(27)$ | 2(27) | (1 12)(2 7)(3 11)(4 10)(5 9)(6 8) | $\begin{pmatrix} v & -1/2 & -u \\ -1/2 & -u & v \\ -u & v & -1/2 \end{pmatrix}$ |
| 57 | $C_2(37)$ | 2(37) | (1 12)(2 8)(3 7)(4 11)(5 10)(6 9) | $\begin{pmatrix} -1/2 & -u & -v \\ -u & v & 1/2 \\ -v & 1/2 & -u \end{pmatrix}$ |
| 58 | $C_2(38)$ | 2(38) | (1 12)(2 9)(3 8)(4 7)(5 11)(6 10) | $\begin{pmatrix} -1 & 0 & 0 \\ 0 & 1 & 0 \\ 0 & 0 & -1 \end{pmatrix}$ |
| 59 | $C_2(48)$ | 2(48) | (1 12)(2 10)(3 9)(4 8)(5 7)(6 11) | $\begin{pmatrix} -1/2 & u & -v \\ u & v & -1/2 \\ -v & -1/2 & -u \end{pmatrix}$ |
| 60 | $C_2(49)$ | 2(49) | (1 12)(2 11)(3 10)(4 9)(5 8)(6 7) | $\begin{pmatrix} v & 1/2 & -u \\ 1/2 & -u & -v \\ -u & -v & -1/2 \end{pmatrix}$ |
| 61 | $C_i$ | $\overline{1}$ | (1 12)(2 9)(3 10)(4 11)(5 7)(6 8) | $\begin{pmatrix} -1 & 0 & 0 \\ 0 & -1 & 0 \\ 0 & 0 & -1 \end{pmatrix}$ |
| 62 | $S_{10}^7(1)$ | $\overline{5}(1)$ | (1 12)(2 8 5 11 3 9 6 7 4 10) | $\begin{pmatrix} -1/2 & u & -v \\ -u & -v & 1/2 \\ -v & -1/2 & -u \end{pmatrix}$ |
| 63 | $S_{10}^7(2)$ | $\overline{5}(2)$ | (1 10 7 4 6 12 3 5 11 8)(2 9) | $\begin{pmatrix} -1/2 & u & v \\ -u & -v & -1/2 \\ v & 1/2 & -u \end{pmatrix}$ |
| 64 | $S_{10}^7(3)$ | $\overline{5}(3)$ | (1 11 8 5 2 12 4 6 7 9)(3 10) | $\begin{pmatrix} -v & 1/2 & -u \\ -1/2 & -u & -v \\ u & -v & -1/2 \end{pmatrix}$ |
| 65 | $S_{10}^7(4)$ | $\overline{5}(4)$ | (1 7 9 6 3 12 5 2 8 10)(4 11) | $\begin{pmatrix} -u & -v & -1/2 \\ -v & -1/2 & u \\ 1/2 & -u & -v \end{pmatrix}$ |
| 66 | $S_{10}^7(5)$ | $\overline{5}(5)$ | (1 8 10 2 4 12 6 3 9 11)(5 7) | $\begin{pmatrix} -u & v & 1/2 \\ v & -1/2 & u \\ -1/2 & -u & -v \end{pmatrix}$ |
| 67 | $S_{10}^7(6)$ | $\overline{5}(6)$ | (1 9 11 3 5 12 2 4 10 7)(6 8) | $\begin{pmatrix} -v & 1/2 & u \\ -1/2 & -u & v \\ -u & v & -1/2 \end{pmatrix}$ |
| 68 | $S_{10}^3(1)$ | $\overline{5}^9(1)$ | (1 12)(2 10 4 7 6 9 3 11 5 8) | $\begin{pmatrix} -1/2 & -u & -v \\ u & -v & -1/2 \\ -v & 1/2 & -u \end{pmatrix}$ |
| 69 | $S_{10}^3(2)$ | $\overline{5}^9(2)$ | (1 8 11 5 3 12 6 4 7 10)(2 9) | $\begin{pmatrix} -1/2 & -u & v \\ u & -v & 1/2 \\ v & -1/2 & -u \end{pmatrix}$ |
| 70 | $S_{10}^3(3)$ | $\overline{5}^9(3)$ | (1 9 7 6 4 12 2 5 8 11)(3 10) | $\begin{pmatrix} -v & -1/2 & u \\ 1/2 & -u & -v \\ -u & -v & -1/2 \end{pmatrix}$ |
| 71 | $S_{10}^3(4)$ | $\overline{5}^9(4)$ | (1 10 8 2 5 12 3 6 9 7)(4 11) | $\begin{pmatrix} -u & -v & 1/2 \\ -v & -1/2 & -u \\ -1/2 & u & -v \end{pmatrix}$ |
| 72 | $S_{10}^3(5)$ | $\overline{5}^9(5)$ | (1 11 9 3 6 12 4 2 10 8)(5 7) | $\begin{pmatrix} -u & v & -1/2 \\ v & -1/2 & -u \\ 1/2 & u & -v \end{pmatrix}$ |
| 73 | $S_{10}^3(6)$ | $\overline{5}^9(6)$ | (1 7 10 4 2 12 5 3 11 9)(6 8) | $\begin{pmatrix} -v & -1/2 & -u \\ 1/2 & -u & v \\ u & v & -1/2 \end{pmatrix}$ |

**Table 4** (*continued*).

| № | Symmetry element | | Cyclic permutation | Rotation matrix |
|---|---|---|---|---|
| 74 | $S_{10}^9(1)$ | $\overline{5}^7(1)$ | (1 12)(2 7 3 8 4 9 5 10 6 11) | $\begin{pmatrix} v & 1/2 & -u \\ -1/2 & u & v \\ -u & -v & -1/2 \end{pmatrix}$ |
| 75 | $S_{10}^9(2)$ | $\overline{5}^7(2)$ | (1 5 6 10 11 12 7 8 3 4)(2 9) | $\begin{pmatrix} v & 1/2 & u \\ -1/2 & u & -v \\ u & v & -1/2 \end{pmatrix}$ |
| 76 | $S_{10}^9(3)$ | $\overline{5}^7(3)$ | (1 6 2 11 7 12 8 9 4 5)(3 10) | $\begin{pmatrix} u & v & -1/2 \\ -v & -1/2 & -u \\ 1/2 & -u & v \end{pmatrix}$ |
| 77 | $S_{10}^9(4)$ | $\overline{5}^7(4)$ | (1 2 3 7 8 12 9 10 5 6)(4 11) | $\begin{pmatrix} -1/2 & -u & -v \\ -u & v & 1/2 \\ v & -1/2 & u \end{pmatrix}$ |
| 78 | $S_{10}^9(5)$ | $\overline{5}^7(5)$ | (1 3 4 8 9 12 10 11 6 2)(5 7) | $\begin{pmatrix} -1/2 & u & v \\ u & v & 1/2 \\ -v & -1/2 & u \end{pmatrix}$ |
| 79 | $S_{10}^9(6)$ | $\overline{5}^7(6)$ | (1 4 5 9 10 12 11 7 2 3)(6 8) | $\begin{pmatrix} u & v & 1/2 \\ -v & -1/2 & u \\ -1/2 & u & v \end{pmatrix}$ |
| 80 | $S_{10}(1)$ | $\overline{5}^3(1)$ | (1 12)(2 11 6 10 5 9 4 8 3 7) | $\begin{pmatrix} v & -1/2 & -u \\ 1/2 & u & -v \\ -u & v & -1/2 \end{pmatrix}$ |
| 81 | $S_{10}(2)$ | $\overline{5}^3(2)$ | (1 4 3 8 7 12 11 10 6 5)(2 9) | $\begin{pmatrix} v & -1/2 & u \\ 1/2 & u & v \\ u & -v & -1/2 \end{pmatrix}$ |
| 82 | $S_{10}(3)$ | $\overline{5}^3(3)$ | (1 5 4 9 8 12 7 11 2 6)(3 10) | $\begin{pmatrix} u & -v & 1/2 \\ v & -1/2 & -u \\ -1/2 & -u & v \end{pmatrix}$ |
| 83 | $S_{10}(4)$ | $\overline{5}^3(4)$ | (1 6 5 10 9 12 8 7 3 2)(4 11) | $\begin{pmatrix} -1/2 & -u & v \\ -u & v & -1/2 \\ -v & 1/2 & u \end{pmatrix}$ |
| 84 | $S_{10}(5)$ | $\overline{5}^3(5)$ | (1 2 6 11 10 12 9 8 4 3)(5 7) | $\begin{pmatrix} -1/2 & u & -v \\ u & v & -1/2 \\ v & 1/2 & u \end{pmatrix}$ |
| 85 | $S_{10}(6)$ | $\overline{5}^3(6)$ | (1 3 2 7 11 12 10 9 5 4)(6 8) | $\begin{pmatrix} u & -v & -1/2 \\ v & -1/2 & u \\ 1/2 & u & v \end{pmatrix}$ |
| 86 | $S_6^5(132)$ | $\overline{3}(132)$ | (1 10 2 12 3 9)(4 5 6 11 7 8) | $\begin{pmatrix} 1/2 & u & -v \\ -u & v & -1/2 \\ v & -1/2 & -u \end{pmatrix}$ |
| 87 | $S_6^5(143)$ | $\overline{3}(143)$ | (1 11 3 12 4 10)(2 7 8 9 5 6) | $\begin{pmatrix} 0 & 0 & -1 \\ -1 & 0 & 0 \\ 0 & -1 & 0 \end{pmatrix}$ |
| 88 | $S_6^5(154)$ | $\overline{3}(154)$ | (1 7 4 12 5 11)(2 3 8 9 10 6) | $\begin{pmatrix} -u & v & -1/2 \\ -v & 1/2 & u \\ -1/2 & -u & v \end{pmatrix}$ |
| 89 | $S_6^5(165)$ | $\overline{3}(165)$ | (1 8 5 12 6 7)(2 3 4 9 10 11) | $\begin{pmatrix} 0 & 1 & 0 \\ 0 & 0 & 1 \\ -1 & 0 & 0 \end{pmatrix}$ |
| 90 | $S_6^5(126)$ | $\overline{3}(126)$ | (1 9 6 12 2 8)(3 4 5 10 11 7) | $\begin{pmatrix} 1/2 & u & v \\ -u & v & 1/2 \\ -v & 1/2 & -u \end{pmatrix}$ |
| 91 | $S_6^5(237)$ | $\overline{3}(237)$ | (1 6 11 12 8 4)(2 10 7 9 3 5) | $\begin{pmatrix} 0 & 1 & 0 \\ 0 & 0 & -1 \\ 1 & 0 & 0 \end{pmatrix}$ |
| 92 | $S_6^5(387)$ | $\overline{3}(387)$ | (1 2 11 12 9 4)(3 6 7 10 8 5) | $\begin{pmatrix} v & 1/2 & -u \\ 1/2 & -u & -v \\ u & v & 1/2 \end{pmatrix}$ |
| 93 | $S_6^5(348)$ | $\overline{3}(348)$ | (1 2 7 12 9 5)(3 11 8 10 4 6) | $\begin{pmatrix} v & -1/2 & -u \\ -1/2 & -u & v \\ u & -v & 1/2 \end{pmatrix}$ |
| 94 | $S_6^5(498)$ | $\overline{3}(498)$ | (1 3 7 12 10 5)(2 8 11 9 6 4) | $\begin{pmatrix} 0 & -1 & 0 \\ 0 & 0 & 1 \\ 1 & 0 & 0 \end{pmatrix}$ |

**Table 4** (*continued*).

| № | Symmetry element | | Cyclic permutation | Rotation matrix |
|---|---|---|---|---|
| 95 | $S_6^5(459)$ | $\overline{3}(459)$ | (1 3 8 12 10 6)(2 4 7 9 11 5) | $\begin{pmatrix} -u & -v & 1/2 \\ v & 1/2 & u \\ 1/2 & -u & v \end{pmatrix}$ |
| 96 | $S_6(132)$ | $\overline{3}^5(132)$ | (1 9 3 12 2 10)(4 8 7 11 6 5) | $\begin{pmatrix} 1/2 & -u & v \\ u & v & -1/2 \\ -v & -1/2 & -u \end{pmatrix}$ |
| 97 | $S_6(143)$ | $\overline{3}^5(143)$ | (1 10 4 12 3 11)(2 6 5 9 8 7) | $\begin{pmatrix} 0 & -1 & 0 \\ 0 & 0 & -1 \\ -1 & 0 & 0 \end{pmatrix}$ |
| 98 | $S_6(154)$ | $\overline{3}^5(154)$ | (1 11 5 12 4 7)(2 6 10 9 8 3) | $\begin{pmatrix} -u & -v & -1/2 \\ v & 1/2 & -u \\ -1/2 & u & v \end{pmatrix}$ |
| 99 | $S_6(165)$ | $\overline{3}^5(165)$ | (1 7 6 12 5 8)(2 11 10 9 4 3) | $\begin{pmatrix} 0 & 0 & -1 \\ 1 & 0 & 0 \\ 0 & 1 & 0 \end{pmatrix}$ |
| 100 | $S_6(126)$ | $\overline{3}^5(126)$ | (1 8 2 12 6 9)(3 7 11 10 5 4) | $\begin{pmatrix} 1/2 & -u & -v \\ u & v & 1/2 \\ v & 1/2 & -u \end{pmatrix}$ |
| 101 | $S_6(237)$ | $\overline{3}^5(237)$ | (1 4 8 12 11 6)(2 5 3 9 7 10) | $\begin{pmatrix} 0 & 0 & 1 \\ 1 & 0 & 0 \\ 0 & -1 & 0 \end{pmatrix}$ |
| 102 | $S_6(387)$ | $\overline{3}^5(387)$ | (1 4 9 12 11 2)(3 5 8 10 7 6) | $\begin{pmatrix} v & 1/2 & u \\ 1/2 & -u & v \\ -u & -v & 1/2 \end{pmatrix}$ |
| 103 | $S_6(348)$ | $\overline{3}^5(348)$ | (1 5 9 12 7 2)(3 6 4 10 8 11) | $\begin{pmatrix} v & -1/2 & u \\ -1/2 & -u & -v \\ -u & v & 1/2 \end{pmatrix}$ |
| 104 | $S_6(498)$ | $\overline{3}^5(498)$ | (1 5 10 12 7 3)(2 4 6 9 11 8) | $\begin{pmatrix} 0 & 0 & 1 \\ -1 & 0 & 0 \\ 0 & 1 & 0 \end{pmatrix}$ |
| 105 | $S_6(459)$ | $\overline{3}^5(459)$ | (1 6 10 12 8 3)(2 5 11 9 7 4) | $\begin{pmatrix} -u & v & 1/2 \\ -v & 1/2 & -u \\ 1/2 & u & v \end{pmatrix}$ |
| 106 | $\sigma(38)$ | $m(38)$ | (1 9)(2 12)(3 8)(4)(5)(6 10)(7)(11) | $\begin{pmatrix} 1 & 0 & 0 \\ 0 & 1 & 0 \\ 0 & 0 & -1 \end{pmatrix}$ |
| 107 | $\sigma(49)$ | $m(49)$ | (1 10)(2 11)(3 12)(4 9)(5)(6)(7)(8) | $\begin{pmatrix} u & -v & -1/2 \\ -v & 1/2 & -u \\ -1/2 & -u & -v \end{pmatrix}$ |
| 108 | $\sigma(37)$ | $m(37)$ | (1 11)(2)(3 7)(4 12)(5 10)(6)(8)(9) | $\begin{pmatrix} -v & -1/2 & -u \\ -1/2 & u & -v \\ -u & -v & 1/2 \end{pmatrix}$ |
| 109 | $\sigma(48)$ | $m(48)$ | (1 7)(2)(3)(4 8)(5 12)(6 11)(9)(10) | $\begin{pmatrix} -v & 1/2 & -u \\ 1/2 & u & v \\ -u & v & 1/2 \end{pmatrix}$ |
| 110 | $\sigma(27)$ | $m(27)$ | (1 8)(2 7)(3)(4)(5 9)(6 12)(10)(11) | $\begin{pmatrix} u & v & -1/2 \\ v & 1/2 & u \\ -1/2 & u & -v \end{pmatrix}$ |
| 111 | $\sigma(15)$ | $m(15)$ | (1 5)(2 10)(3 9)(4)(6)(7 12)(8)(11) | $\begin{pmatrix} u & v & 1/2 \\ v & 1/2 & -u \\ 1/2 & -u & -v \end{pmatrix}$ |
| 112 | $\sigma(16)$ | $m(16)$ | (1 6)(2)(3 11)(4 10)(5)(7)(8 12)(9) | $\begin{pmatrix} 1/2 & -u & -v \\ -u & -v & -1/2 \\ -v & -1/2 & u \end{pmatrix}$ |
| 113 | $\sigma(12)$ | $m(12)$ | (1 2)(3)(4 7)(5 11)(6)(8)(9 12)(10) | $\begin{pmatrix} -1 & 0 & 0 \\ 0 & 1 & 0 \\ 0 & 0 & 1 \end{pmatrix}$ |
| 114 | $\sigma(13)$ | $m(13)$ | (1 3)(2)(4)(5 8)(6 7)(9)(10 12)(11) | $\begin{pmatrix} 1/2 & u & -v \\ u & -v & 1/2 \\ -v & 1/2 & u \end{pmatrix}$ |

**Table 4** (*continued*).

| № | Symmetry element | | Cyclic permutation | Rotation matrix |
|---|---|---|---|---|
| 115 | $\sigma(14)$ | $m(14)$ | (1 4)(2 8)(3)(5)(6 9)(7)(10)(11 12) | $\begin{pmatrix} u & -v & 1/2 \\ -v & 1/2 & u \\ 1/2 & u & -v \end{pmatrix}$ |
| 116 | $\sigma(34)$ | $m(34)$ | (1)(2 5)(3 4)(6)(7 9)(8)(10 11)(12) | $\begin{pmatrix} -v & 1/2 & u \\ 1/2 & u & -v \\ u & -v & 1/2 \end{pmatrix}$ |
| 117 | $\sigma(26)$ | $m(26)$ | (1)(2 6)(3 5)(4)(7 10)(8 9)(11)(12) | $\begin{pmatrix} 1/2 & u & v \\ u & -v & -1/2 \\ v & -1/2 & u \end{pmatrix}$ |
| 118 | $\sigma(45)$ | $m(45)$ | (1)(2)(3 6)(4 5)(7 11)(8 10)(9)(12) | $\begin{pmatrix} 1 & 0 & 0 \\ 0 & -1 & 0 \\ 0 & 0 & 1 \end{pmatrix}$ |
| 119 | $\sigma(23)$ | $m(23)$ | (1)(2 3)(4 6)(5)(7)(8 11)(9 10)(12) | $\begin{pmatrix} 1/2 & -u & v \\ -u & -v & 1/2 \\ v & 1/2 & u \end{pmatrix}$ |
| 120 | $\sigma(56)$ | $m(56)$ | (1)(2 4)(3)(5 6)(7 8)(9 11)(10)(12) | $\begin{pmatrix} -v & -1/2 & u \\ -1/2 & u & v \\ u & v & 1/2 \end{pmatrix}$ |